

This document is confidential and is proprietary to the American Chemical Society and its authors. Do not copy or disclose without written permission. If you have received this item in error, notify the sender and delete all copies.

**Design, Synthesis and Evaluation of Thyronamine Analogues
as Novel Potent Mouse Trace Amine Associated Receptor 1
(mTAAR1) Agonists**

Journal:	<i>Journal of Medicinal Chemistry</i>
Manuscript ID:	jm-2015-005267.R2
Manuscript Type:	Article
Date Submitted by the Author:	26-May-2015
Complete List of Authors:	Chiellini, Grazia; Università Pisa, Nesi, Giulia; Università di Pisa, Digiacomo, Maria; Università di Pisa, Malvasi, Rossella; Università di Pisa, Espinoza, Stefano; Istituto Italiano di Tecnologia, Genova,, Sabatini, Martina; Università Pisa, Frascarelli, Sabina; Università Pisa, Laurino, Annunziata; università degli studi di firenze, neurofarba Cichero, Elena; University of Genoa, Macchia, Marco; Università di Pisa, Gainetdinov, Raul; Istituto Italiano di Tecnologia, Genova,, Fossa, Paola; University of Genova, Scienze Farmaceutiche Raimondi, Laura; University of Florence, Zucchi, Riccardo; Università Pisa, Rapposelli, Simona; Università di Pisa, Dipartimento di Farmacia

SCHOLARONE™
Manuscripts

1
2
3 **Design, Synthesis and Evaluation of Thyronamine Analogues as Novel Potent Mouse**
4
5 **Trace Amine Associated Receptor 1 (*m*TAAR1) Agonists**
6
7

8
9 Grazia Chiellini^{1*}, Giulia Nesi², Maria Digiacomo², Rossella Malvasi², Stefano
10 Espinoza³, Martina Sabatini¹, Sabina Frascarelli¹, Annunziatina Laurino⁴, Elena Cichero⁵,
11 Marco Macchia², Raul. R. Gainetdinov^{6,7}, Paola Fossa⁵, Laura Raimondi⁴, Riccardo
12 Zucchi¹, Simona Rapposelli^{2*}.
13
14
15
16
17

18
19 ¹*Dept. of Pathology, University of Pisa, Pisa, Italy*, ²*Dept. of Pharmacy, University of*
20 *Pisa, Pisa, Italy*, ³*Department of Neuroscience and Brain Technologies, Istituto Italiano*
21 *di Tecnologia, Genova, Italy*, ⁴*Dept. of NEUROFARBA; Section of Pharmacology,*
22 *University of Florence, Italy*, ⁵*Dept. of Pharmacy, University of Genoa, Genoa, Italy.*
23
24 ⁶*Institute of Translational Biomedicine, St. Petersburg State University, St. Petersburg,*
25 *199034, Russia*, ⁷*Skolkovo Institute of Science and Technology (Skoltech) Skolkovo,*
26 *Moscow region, 143025, Russia.*
27
28
29
30
31
32
33
34
35
36
37
38
39

40 **Keywords:** *m*TAAR1 agonist; Trace amine associated receptor 1; Thyronamine; T1AM;
41
42 T0AM
43
44
45
46
47

48 **Abstract**
49

50
51
52 Trace amine associated receptor 1 (TAAR1) is a GPCR expressed in brain and
53 periphery activated by a wide spectrum of agonists that include, but are not limited to,
54 trace amines (TAs), amphetamine-like psychostimulants and endogenous thyronamines,
55
56
57
58
59
60

1
2
3 such as thyronamine (T0AM) and 3-iodothyronamine (T1AM). Such polypharmacology
4
5 has made it challenging to understand the role and the biology of TAAR1. In an effort to
6
7 understand the molecular basis of TAAR1 activation, we rationally designed and
8
9 synthesized a small family of thyronamine derivatives. Among them, compounds **2** and **3**
10
11 appeared to be a good mimic of the parent endogenous thyronamine, T0AM and T1AM
12
13 respectively, both *in vitro* and *in vivo*. Thus, these compounds offer suitable tools for
14
15 studying the physiological roles of mouse TAAR1, and could represent the starting point
16
17 for the development of more potent and selective TAAR1 ligands.
18
19
20
21
22

23 **Introduction**

24
25
26 Thyronamines (TAMs) are naturally occurring signaling compounds, originally
27
28 postulated to derive from thyroid hormone (T4) throughout deiodination and
29
30 decarboxylation¹. Although these compounds were first described almost seven decades
31
32 ago, their importance was not recognized until 2004, when Scanlan's group identified
33
34 them as potential ligands of the trace amine associated receptor 1 (TAAR1)¹. So far, two
35
36 representatives of TAMs, namely 3-iodothyronamine (T1AM) and thyronamine (T0AM)
37
38 (Figure 1), have been detected *in vivo*, with T1AM being the most abundant¹⁻².
39
40
41
42
43
44
45
46
47
48
49
50
51
52
53
54
55
56
57
58
59
60

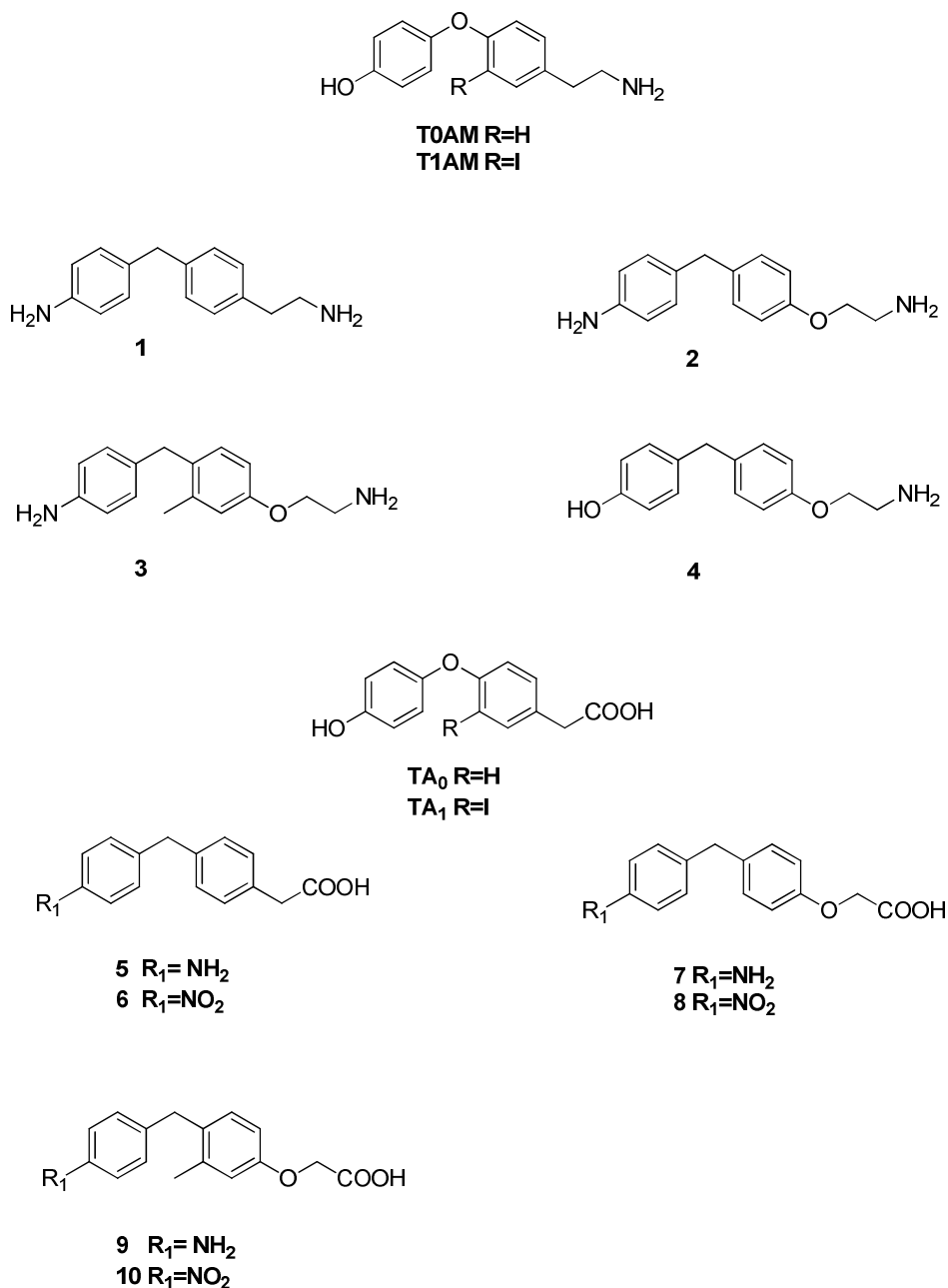


Figure 1. Structures of endogenous thyronamines and new synthetic analogues.

T1AM has been detected in human blood and virtually in every tissue in rodents, at concentrations on the order of a few pmol/g. The pathway responsible for T1AM biosynthesis is still unclear. In human patients subjected to thyroidectomy and undergoing replacement therapy with oral thyroxine, plasma T1AM levels were reported

1
2
3 to be normal, suggesting peripheral conversion of T4 to T1AM³. However, T1AM
4
5 decreased in rat liver after treatment with perchlorate and methimazole, but liver
6
7 concentration was not normalized after i.p. treatment with exogenous T4, suggesting that
8
9 T1AM is produced by the thyroid gland and is not an extra-thyroidal metabolite of T4⁴. A
10
11 preliminary evidence on the T4 conversion into T1AM on an everted gut sac model has
12
13 been recently reported⁵.
14
15
16

17
18 T1AM should be regarded as a chemical messenger, since it interacts with
19
20 specific receptors and produces significant functional effects. T1AM is not a ligand for
21
22 nuclear thyroid hormone receptors (TRs), instead it stimulates with nanomolar affinity
23
24 TAAR1, which is the best characterized TAAR member, found in specific areas of the
25
26 central nervous system as well as in certain peripheral tissues⁶⁻¹⁰. Recent evidence gained
27
28 by using transgenic animals and newly developed pharmacological tools indicates that
29
30 targeting TAAR1 may provide new therapeutic approach for a range of neuropsychiatric
31
32 and metabolic disorders⁶ T1AM binding to TAAR1 engages G α_s -type G proteins that
33
34 activate adenylyl cyclases¹, but notably, this compound also interacts with amine
35
36 transporters, with mitochondrial proteins, and binds with high affinity to apoB100¹¹.
37
38 Recently, an inverse agonistic action at TAAR5 has also been described¹².
39
40 Administration of exogenous T1AM to rodents caused transient decrease in body
41
42 temperature and reduction of cardiac inotropic and chronotropic state^{1, 13, 14}. While these
43
44 effects occurred at micromolar concentration, metabolic and neurological effects were
45
46 observed at lower dosages, which increased endogenous tissue concentration by about
47
48 one order of magnitude¹⁵.
49
50
51
52
53
54
55
56
57
58
59
60

1
2
3 T1AM favors fatty acid oxidation over carbohydrate oxidation¹⁶⁻¹⁷, and chronic
4 treatment with exogenous T1AM in obese mice produced a significant reduction in body
5 weight, in the absence of changes in food consumption¹⁷. T1AM has also been reported
6 to have neuromodulatory effects, since i.c.v. administration in mice elicited pro-learning
7 and anti-amnestic effects¹⁸. Intracerebral injection also produced hormonal changes, i.e.
8 stimulation of glucagon and inhibition of insulin secretion¹⁹⁻²¹ and modifications of
9 alimentary behavior²². Although its physiological function remains elusive, T1AM has
10 already revealed promising therapeutic potential. Noteworthy, the structural similarities
11 between thyroxine, T1AM, and monoamine neurotransmitters suggest an intriguing role
12 for T1AM as both a neuromodulator and a hormone-like molecule that may constitute a
13 part of thyroid hormone action.
14
15
16
17
18
19
20
21
22
23
24
25
26
27
28
29

30 All these findings convey that this molecule may have great potential for a wide
31 variety of therapeutic applications, such as obesity, weight loss, neuro-psychiatric
32 disorders and cancer. Unfortunately, thyronamines are rapidly metabolized by different
33 enzyme systems such as amino-oxidase (MAO, SSAO), deiodinases (DIO3),
34 sulfotransferases (SULT1A1 and SULT1A3), N-acetyltransferases and glucuronidases²³⁻
35
36
37
38
39
40
41
42
43
44
45
46
47
48
49
50
51
52
53
54
55
56
57
58
59
60
24 and that can obviously constitute a limit to their therapeutic use.

Consequently, the great therapeutic potential as well as the lack of new tools to
elucidate T1AM physiological function urge the development of novel synthetic
analogues of T1AM.

Herein, we describe the synthesis and properties of a small series (**1-10**) of new
synthetic analogues of thyronamines (Figure 1). These compounds were screened *in vitro*

1
2
3 for TAAR1 activation, and selected compounds were evaluated *in vivo* to characterize
4 their functional and metabolic effects. Furthermore, to rationalize the pharmacological
5 results and to support and guide the synthetic efforts, *in silico* docking studies on
6 compounds T₁AM and **1-10** were also performed in order to simulate the interaction of
7 the synthesized compounds with the putative receptor-binding site. Given the absence of
8 crystallographic data for the TAAR1 receptor, a theoretical model of the *m*TAAR1
9 receptor was built to carry out the docking studies.
10
11
12
13
14
15
16
17
18
19

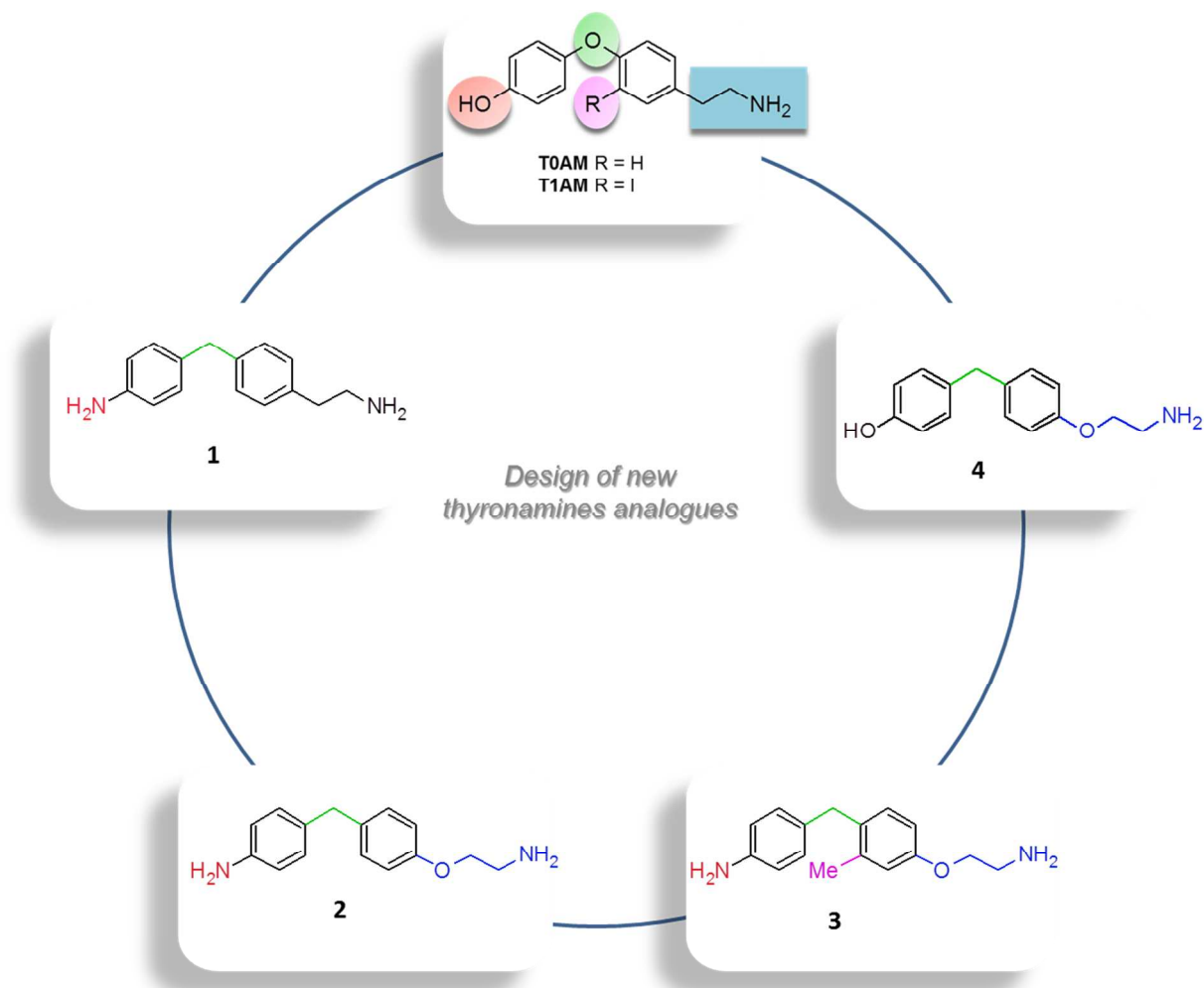
20
21 Following a multidisciplinary approach, we identified two compounds, namely **2**
22 and **3** that are equipotent to endogenous thyronamines, and could represent suitable tools
23 for studying the physiological roles of TAAR1 receptor using *in vitro* and/or *in vivo*
24 models.
25
26
27
28
29
30

31 **Results and Discussion**

32
33
34 **Rational design of new compounds.** The recent discovery that endogenous
35 thyronamines (i.e. T₀AM and T₁AM) potently activate rat TAAR1 (*r*TAAR1) and mouse
36 TAAR1 (*m*TAAR1) heterologously expressed in HEK293 cells, with T₁AM being the
37 most effective, spurred the discovery of the first rationally designed “superagonist” and
38 antagonist compounds that target TAAR1²⁵. In general, structural-activity relationship
39 studies have led to the following conclusions: a basic amino group at C α is required for
40 activity, and monomethylation of the amine can be beneficial; an iodide or methyl
41 substituent at the 3-position of the thyronamine scaffold is optimal for activity; the 4'-OH
42 of thyronamine is not necessary for activity but its removal may render the remaining
43 compound difficult to metabolize and possibly result in impaired clearance.
44
45
46
47
48
49
50
51
52
53
54
55
56
57
58
59
60

1
2
3 With the aim of enriching the number of selective ligands for TAAR1, and providing new
4 tools to facilitate the understanding of TAAR1 physiological functions and therapeutic
5 potential, in the present work we designed and synthesized a novel class of thyronamine
6 analogs that are more synthetically accessible than traditional thyronamines and have
7 potentially useful receptor activation and functional properties.
8
9

10
11
12
13
14
15
16 It is well known that biaryl-ether-forming reactions represent a significant problem in
17 organic synthesis, and the biaryl-ether linkage in thyronamines requires the construction
18 of both the appropriate boronic acid and phenol fragments throughout a multi steps
19 process²⁶. Thus, taking advantage of our knowledge in the synthesis of analogues of
20 thyroid hormones²⁷, we first simplified the chemical synthesis of thyronamine analogues
21 by replacing the oxygen bridging the aromatic rings with a methylene linkage.
22
23
24
25
26
27
28
29
30
31
32
33
34
35
36
37
38
39
40
41
42
43
44
45
46
47
48
49
50
51
52
53
54
55
56
57
58
59
60
Subsequently, we examined the possibility of replacing the 4'-OH substituent of
thyronamines with a bioisostere group, such as the 4'-NH₂, which retains the same H-
bonding donor and acceptor capabilities of the OH group, while also improving the
pharmacokinetic properties of the molecule (i.e. solubility, hydrophilicity). Following
this approach we obtained the first oxygen free biaryl-methane thyronamine analog **1**
(Figure 2).



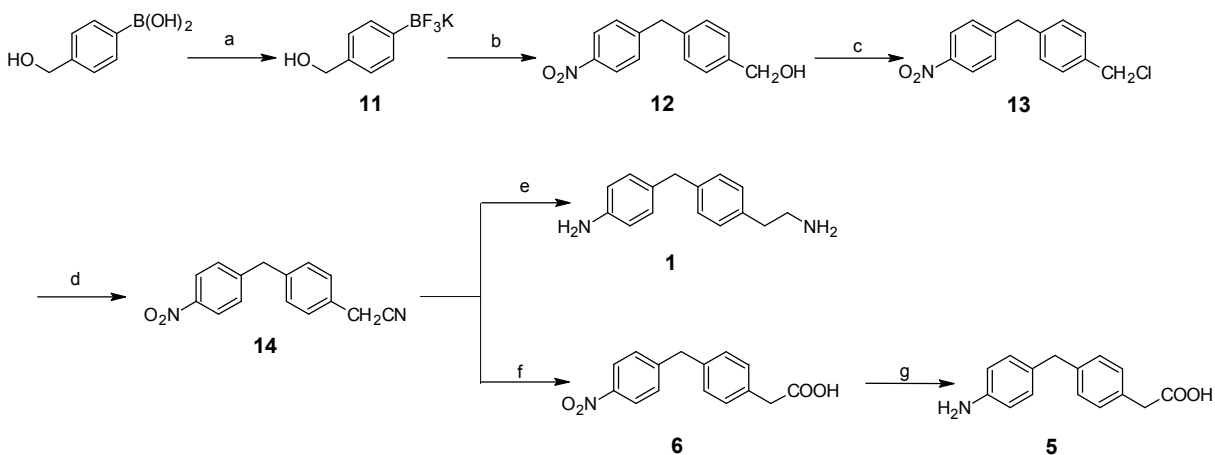
38 **Figure 2.** Medicinal chemistry strategies pursued in the design of new thyronamine
39 analogues.
40
41

42
43 In addition, given the pharmacological survey by Bunzow et al.⁸ showing that TAAR1
44 could be activated by aminergic GPCR drugs with structurally diverse ethylamine
45 segments, and knowing that the ethylamine side chain of thyronamines is exposed to
46 rapid metabolic degradation by MAO²³, we decided to synthesize new thyronamine
47 analogs by replacing the ethylamine side chain with an aminoethoxy group. Thus, three
48 new aminoethoxy analogs of our scaffold compound **1** were designed (Figure 2), with **2**
49
50
51
52
53
54
55
56
57
58
59
60

1
2
3 and **4** being a close mimic of thyronamine (T0AM), whereas **3** compound, which has a
4
5 methyl group at position 3, could be considered a new halogen free 3-iodothyronamine
6
7 (T1AM) analog.
8
9

10
11 Oxidative deamination followed by aldehyde oxidation by ubiquitous enzyme aldehyde
12
13 dehydrogenase is a major and rapid pathway of T1AM and T0AM metabolism, resulting
14
15 in the production of the corresponding thyroacetic acids, namely TA₁ and TA₀²³ (Figure
16
17 1). This conversion could be significantly inhibited by treatment with the monamine
18
19 oxidase (MAO) and semicarbazide-sensitive amine oxidase (SSAO) inhibitor,
20
21 iproniazid²³. Recent findings suggested that generation of TA₁ by deamination might
22
23 contribute, at least in part, to the acute effects of T1AM *in vivo* and showed that oxidative
24
25 deamination had a marked effect on T1AM pharmacokinetics²⁰. Thus, in order to expand
26
27 our SAR analysis on 4'-NH₂-biaryl-methane thyronamine analogues, we synthesized the
28
29 corresponding deamination product of compounds **1-3**, namely **5**, **7** and **9**, as well as their
30
31 4'-NO₂ analogues, namely **6**, **8** and **10**(Figure 1).
32
33
34
35
36
37

38 **Synthesis.** Utilizing a divergent synthetic route, we synthesized the entire panel of new
39
40 thyronamine analogues (**1-10**) from commercially available starting materials.
41
42
43
44
45
46
47
48
49
50
51
52
53
54
55
56
57
58
59
60

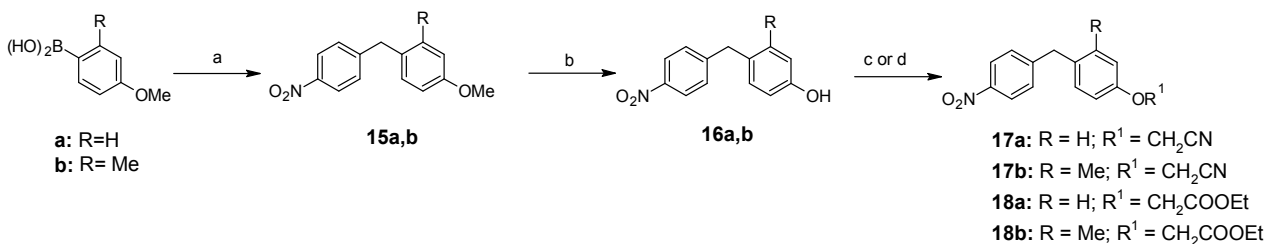
Scheme 1^a

^a**Reagents and conditions:** a: KHF_2 , $\text{MeOH}/\text{H}_2\text{O}$, rt, 30'; b: 4-Nitrobenzylbromide, PdCl_2 dppf, Cs_2CO_3 , $\text{H}_2\text{O}/\text{Dioxane}$, 95°C , 24 h; c: SOCl_2 , CHCl_3 , rt, 2h; d: NaCN , $\text{H}_2\text{O}/\text{CH}_3\text{CN}$, mw; e: LiAlH_4 , AlCl_3 , THF, reflux, 12 h; f: H_2SO_4 50%, reflux, 30'; g: Hydrazine hydrate, Carbon, FeCl_3 , MeOH , reflux, 12 h.

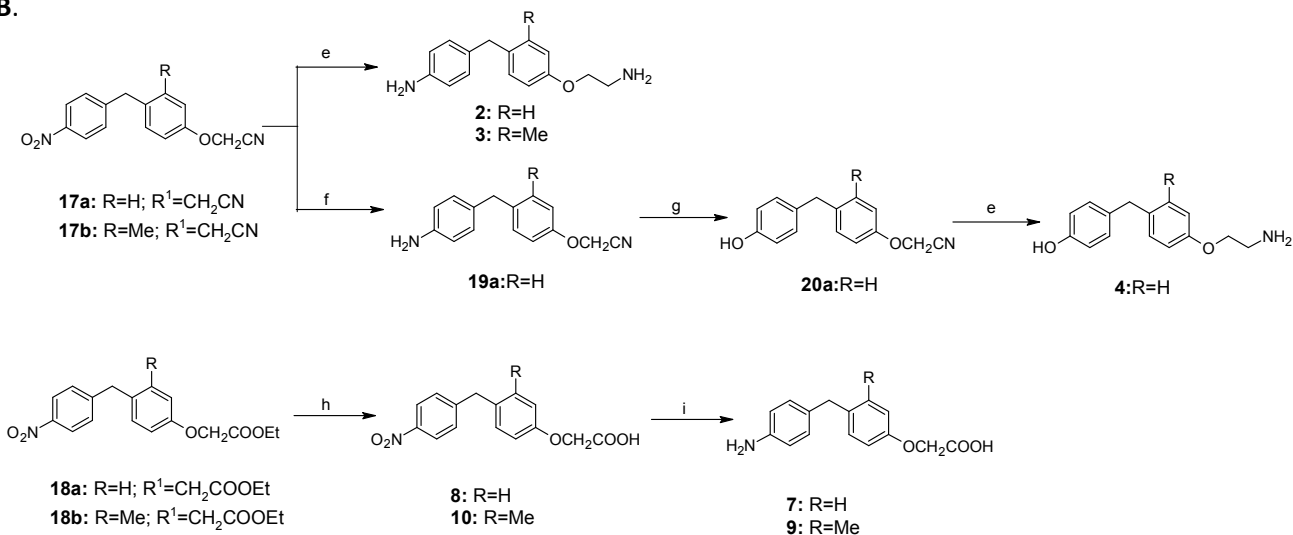
Palladium-catalyzed Suzuki-Miyaura coupling of p-nitrobenzyl bromide with selected phenyl boronic acid derivatives, either commercially available or easily generated *in situ*, was a crucial component to our synthetic route, and allow to efficiently produce the key biaryl methane intermediates **12** and **15a,b** in only one to two steps. As shown in Scheme 1, starting from intermediate **12**, easily obtained by palladium(0)-catalyzed Suzuki-Miyaura cross-coupling reaction of the trifluoroborate salt **11** with 4-nitrobenzyl bromide²⁸, the reaction with SOCl_2 followed by the nucleophilic substitution with NaCN gave the nitrile derivative **14**. The reduction of **14** with LiAlH_4 in the presence of a Lewis's acid afforded the diamine **1**, while its hydrolysis with H_2SO_4 50% provided the carboxylic acid **6**. The reduction of **6** with hydrazine hydrate in the presence of FeCl_3 and carbon provided the corresponding 4-(4-aminobenzyl)phenylacetic acid **5**.

Scheme 2^a

A.



B.



Reagents and conditions: **a:** 4-Nitrobenzyl bromide, K₂CO₃, PdCl₂, Acetone/H₂O, rt, 72 h; **b:** BBr₃, DCM, 0°C, 1 h; **c:** BrCH₂CN, DMF, Cs₂CO₃, rt, 30'; **d:** BrCH₂COOEt, DMF, Cs₂CO₃, rt, 30'; **e:** LiAlH₄, AlCl₃, THF, reflux, 12 h; **f:** H₂, Pd/C, AcOH, EtOH, rt, 12 h; **g:** NaNO₂, H₂SO₄, H₂O, 100°C, 1h; **h:** NaOH 10%, MeOH, reflux, 1h; **i:** Hydrazine hydrate, Carbon, FeCl₃, MeOH, reflux, 12 h.

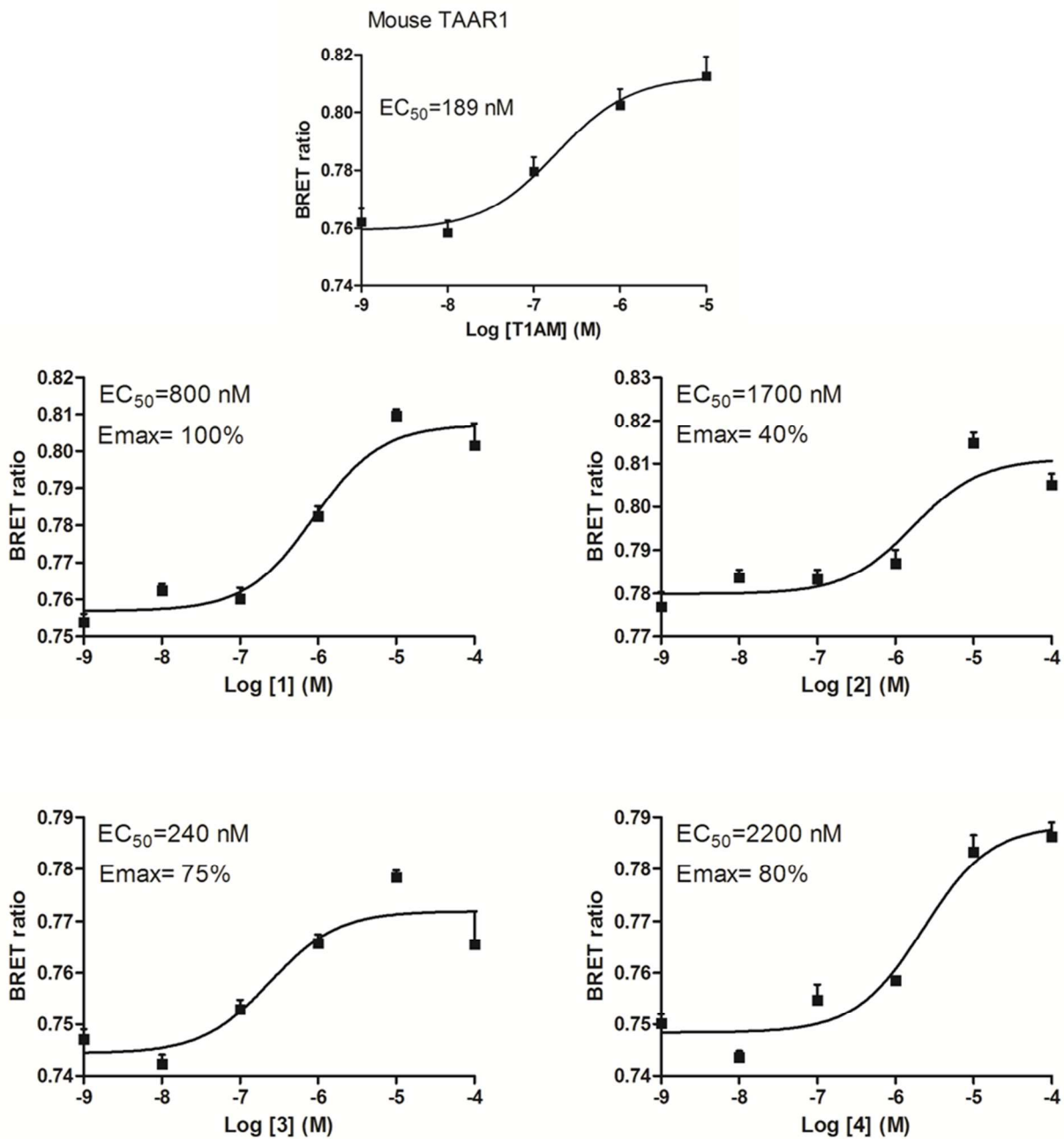
Palladium(0)-catalyzed Suzuki-Miyaura cross-coupling reaction between the *p*-nitrobenzylbromide and the appropriate 4-methoxyboronic acid, provided the compound **15a,b** (Scheme 2, panel A). The resulting adduct was treated with boron tribromide to obtain the phenolic derivative **16a,b**, which was then alkylated using bromoacetonitrile or ethyl bromoacetate affording compound **17a,b** or **18a,b**, respectively. The final products **2** and **3** were obtained by reduction with LiAlH₄/AlCl₃ of **17a** and **17b**, respectively

1
2
3 (Scheme 2, panel B). The catalytic hydrogenation of **17a** followed by the reaction with
4
5 NaNO₂ in H₂SO₄ gave the phenol **20a** which was reduced with LiAlH₄/AlCl₃ to provide
6
7 the desired product **4**. Finally, the cleavage of ethyl ester **18a,b** afforded the final
8
9 products **8** and **10** which were submitted to reduction with hydrazine hydrate in the
10
11 presence of FeCl₃ and carbon to afford the amines **7** and **9**.
12
13

14
15
16 The newly designed compounds were then tested on the basis of the pharmacological
17
18 responses originally described for T0AM and T1AM, namely cAMP production in HEK-
19
20 293 cells expressing *mTAAR1*, induction of negative inotropic effect (reduced cardiac
21
22 output) in isolated working rat heart preparations, and modulation of plasma glucose
23
24 level in CD-1 mice.
25
26

27
28 **Receptor activation.** As previously reported, both *rTAAR1* and *mTAAR1* are coupled to
29
30 stimulatory G proteins and thus induce cAMP production in HEK293 stable cell lines
31
32 upon agonist exposure⁸. We measured the activity of the new compounds using BRET
33
34 based assay²⁹ in which HEK293 cells were transfected with *mTAAR1*, or empty vector as
35
36 control, and the cAMP BRET biosensor³⁰. As reference compound we used the standard
37
38 TAAR1 agonist β-PEA that in our tests also increased cAMP through TAAR1 activation
39
40 (EC₅₀=138 nM). In the initial screening phase, all the compounds were tested at 10 μM
41
42 either for agonistic or antagonistic activity. For the compounds that were found to be
43
44 active, a dose response was then performed to calculate their corresponding EC₅₀ values.
45
46 After the initial phase, only the four biaryl-methane thyronamine analogues **1-4**, were
47
48 found to potently activate TAAR1. As shown in Figure 3, compounds **1-4** are effective
49
50 TAAR1 agonists in HEK-293 cells transfected with *mTAAR1*, and compound **3**, which
51
52 shares a close similarity to T1AM, was found to be the most potent (**3**: EC₅₀ = 240 nM;
53
54
55
56
57
58
59
60

1
2
3 T1AM $EC_{50} = 189$ nM). Noteworthy, even though **1** resulted to be less potent than **3**
4
5
6 ($EC_{50} = 800$ nM) it shows the highest efficacy ($E_{max} = 100\%$).
7
8
9



1
2
3 **Figure 3.** cAMP variations induced by the tested compounds in cells co-expressing
4 *m*TAAR1 and EPAC. Cells were treated with the compounds at different concentrations
5 and plotted as a dose–response experiment. Curve was fitted using a nonlinear regression
6 and one site specific binding with GraphPad Prism5. Data are plotted as SEM of 4-5
7 independent experiments.
8
9
10
11

12
13
14
15
16 **Heart perfusion experiments.** It is already known that endogenous thyronamines (i.e.
17 T0AM and T1AM) produced a reversible, dose-dependent negative inotropic effect in the
18 isolated working rat heart preparations, and recent studies have shown the expression of
19 mRNA coding for at least five different TAAR subtypes in rat heart, namely TAAR1-4
20 and TAAR8a, with the latter being quantitatively preponderant¹³⁻¹⁴. The T1AM
21 corresponding synthetic analog **3**, which has emerged from the TAAR1 activation study
22 as the most potent derivative, and the T0AM relative synthetic compound **2**, were also
23 examined in heart perfusion experiments. Freshly isolated adult rat hearts were perfused
24 with buffer containing escalating doses of **2** or **3**, while the hemodynamic variables were
25 monitored. **3** doses between 20 and 40 μ M led to an immediate reduction in cardiac
26 output (Figure 4).
27
28
29
30
31
32
33
34
35
36
37
38
39
40
41
42
43
44
45
46
47
48
49
50
51
52
53
54
55
56
57
58
59
60

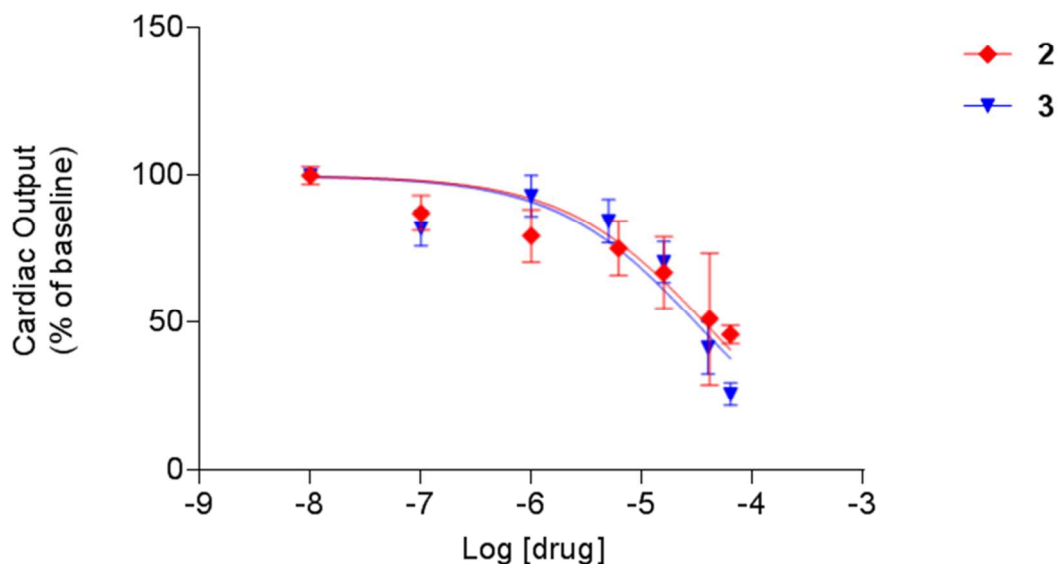


Figure 4. Dose-response curves for the effects of **2** (red) and **3** (blue) on cardiac output. Data points are values measured after 30 min of perfusion, expressed as percentage of baseline values. Bars are mean \pm SE of 3–7 hearts per group. Results were analyzed by nonlinear regression using a sigmoidal dose response model to calculate the reported IC₅₀'s values.

Within 10 min of receiving the highest **3** dose (40 μ M), cardiac output dropped by 60%, as compared with controls, and remained at this rate for the duration of the experiment (1 h). The IC₅₀ averaged 30 μ M for the effect on cardiac output being almost comparable to previously observed T1AM IC₅₀ value (i.e IC₅₀ = 27 μ M), while only minor effects were observed on heart rate. In isolated rat hearts with reduced inotropic drive resulting from pretreatment with **3**, administration of isoproterenol increased cardiac output (data not shown). This normalizing response to isoproterenol shows that β -adrenergic signaling is conserved in the presence of **3**, thus suggesting that the regulation of cardiac function is under the control of signaling pathways modulated by norepinephrine-sensitive and

1
2
3 thyronamine-sensitive G protein coupled receptors (GPCRs). **2** treatment also resulted in
4 a rapid reduction in cardiac output with no observable effect on heart rate, suggesting that
5
6 also **2** is a negative inotropic agent with an IC_{50} of 34 μ M, as compared with 30 μ M for **3**
7
8 (Figure 4).
9
10

11
12
13 Rat hearts were also perfused with buffer containing escalating doses (1-100 μ M) of **7**
14 and **9**, which represent the potential deamination product of **2** and **3**, respectively, but no
15
16 effects on cardiac function were observed (data not shown).
17
18
19

20
21 **Modulation of plasma glucose level.** T1AM has been reported to induce glucagon
22 secretion and determine insulin secretion. These effects were observed with i.c.v.
23 administration of T1AM dosages at low as 1.3 μ g/kg¹⁹⁻²⁰, but evidence for a peripheral
24
25 action has also be reported at higher dosages^{21, 31}.
26
27
28
29
30
31

32 Consequently, the effects induced by **2** and **3** derivatives on plasma glucose level were
33 also assessed. Figure 5 shows that a single low dose of **2** (1.32 μ g/kg, ip) or **3** (4.0 μ g/kg,
34 ip) increases plasma glycaemia with a potency comparable to that of T0AM and T1AM,
35
36 respectively.
37
38
39
40
41
42
43
44
45
46
47
48
49
50
51
52
53
54
55
56
57
58
59
60

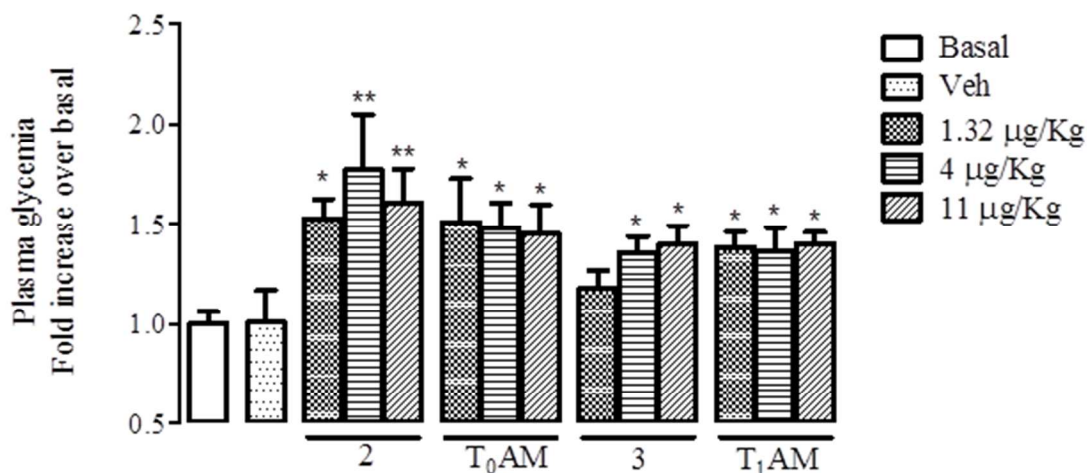


Figure 5. Effect of **2** and **3** on plasma glycaemia in comparison to T₀AM and T₁AM, respectively. *P < 0.05 vs. vehicle. **P < 0.001 vs. vehicle.

Molecular modeling

In order to explore the *m*TAAR1 binding site features, a homology model was built using the ligand-based homology modeling strategy proposed by Moro³². Briefly, the ligand-based homology modeling is performed by the proper handling of insertions and deletions of any selected extra-atoms during the energy tests and minimization stages of the modeling procedure. This computational option is very useful when one wishes to build a homology model in the presence of a ligand docked into the primary template and has been widely and fruitfully used by us to build GPCR as well as various enzyme models³³⁻³⁴. More specifically, in this work the GPCR 3D structure was generated using

3PDS β_2 -adrenoreceptor as template, following the procedure we previously applied for the development of the human TAAR1 model³³

Similarly, the *m*TAAR1 model was built and refined in the presence of T1AM properly placed into the 3PDS β_2 -adrenoreceptor binding site by docking procedures. In this way, we can safely assume that we were able to build a much better *m*TAAR1 binding site for the *in silico* analysis of the new derivatives than using standard homology modeling protocols. More specifically, starting from the derived β_2 -adrenoreceptor/agonist complex, the *m*TAAR1 model was derived by aligning the *m*TAAR1 (Q923Y8) fast a sequence onto the 3PDS X-ray coordinates, using the Blosum62 matrix implemented in MOE software (Figure 6a).

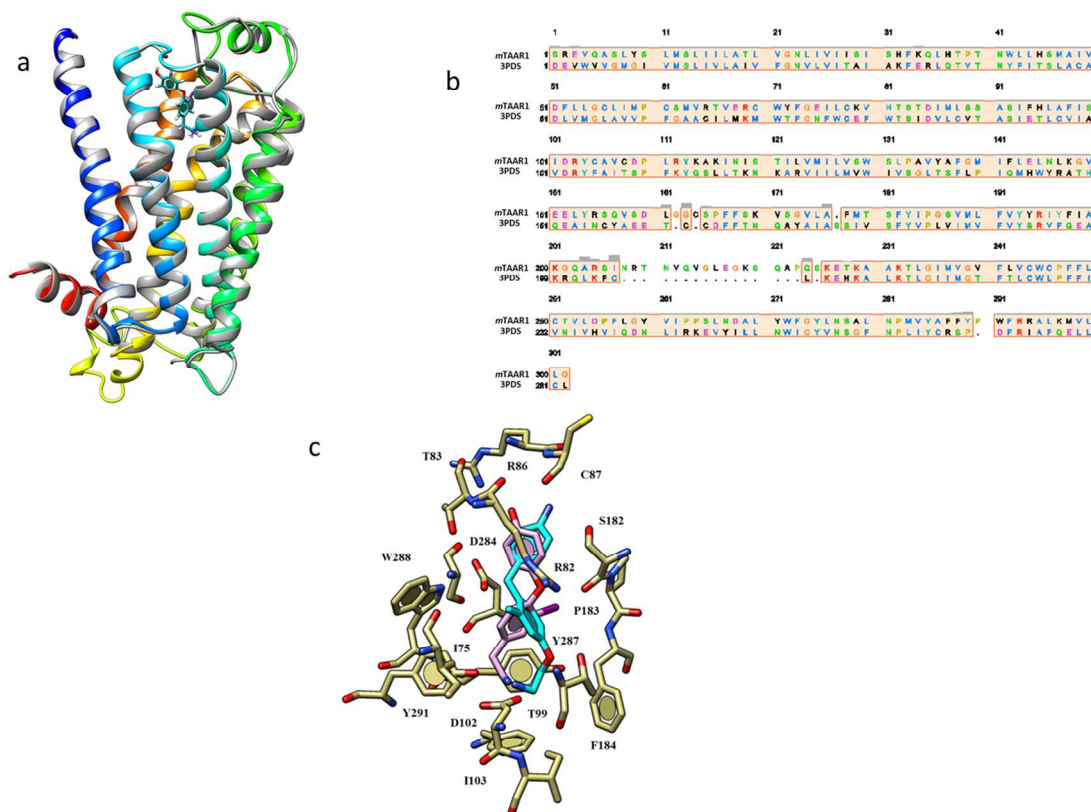


Figure 6 a. The superimposition of the final *mTAAR1* model (backbone colored by rainbow) on the 3PDS coordinates (backbone in grey) is depicted. The T1AM structure is also reported in stick (colored by atom type, C atom: cyan). **b.** Sequence alignment of the *mTAAR1* on the basis of the human β_2 -adrenoreceptor (pdb: 3PDS) coordinated. **c.** Docking mode of the T₁AM and of thyronamine analogue **3** into the putative *mTAAR1* binding site. The ligands are reported in stick, colored by atom type (C atom: pink and cyan, respectively)

The reliability of the alignment was verified by the high value of the pairwise percentage residue identity (PPRI = 33%). Accordingly, a consistent number of *mTAAR1* residues resulted to be conserved in comparison with those of the β_2 -adrenoreceptor TM helices : (i) M29, L31, L34, G39, V43, I47, S30, I32, A35, N40, I44, F50, L53 in TM1, (ii) T57, N58, S63, A65, D68, G72, P77 in TM2, (iii) C95, T99, S100, D102, A108, S109, I110, L113, I116, D119, R120, Y121 in TM3 (the DRY motif; 119-121 residues), (iv) V141, I143, L144, W147, F155, I157 in TM4, (v) A193, S197, F198, Y199, P201, M205, F207, V208, Y209, R211, A216, K217 in TM5, (vi) K242, E243, K245, A246, K248, T249, L250, G251, I252, G255, F257, C260, W261, P263, F264, F265 in TM6 (CWXP motif; 260-263 residues); (vii) L286, W288, G290, Y291, N293, S294, N297, P298, Y301 in TM7.

The derived backbone conformation was inspected by Ramachandran plot (showing absence of outliers) and superimposed to the coordinates of the template structure (RMSD = 0.459 Å; Figure 6b).

Subsequently, we used our *mTAAR1* model to perform docking studies on the reference compound T₁AM and on **1-10** derivatives.

1
2
3 On the basis of our calculations, **T1AM** proved to be highly stabilized into the receptor
4 binding site by two H-bonds between the protonated amine group and the D102 and
5 Y291 side-chains, and also by one H-bond between the phenolic hydroxyl group and the
6 R82 backbone carbonyl moiety. Furthermore, the T1AM protonated amine group is able
7 to establish additional cation- π contacts with Y287 and with the aforementioned Y291.
8 Notably, the central ether oxygen seems not to be involved in any significant aminoacid
9 interaction (Figure 6c).
10
11
12
13
14
15
16
17
18
19

20 The **2,3** and **1,4** derivatives, partially shared the T1AM docking mode, described above.
21 In particular, **3** (being the most active of this series) displayed: (i) two H-bonds between
22 the protonated amine group and the D102 and Y291 side chains, (ii) cation- π interactions
23 between the same group and Y291, (iii) π - π stacking between the 4-(2-
24 aminoethoxy)phenyl group of the molecule and Y287 (Figure 6c). In addition, the
25 aniline portion projects toward the R86 side chain, establishing cation- π interactions,
26 while no H-bonds with the R82 backbone oxygen atom were detected. Notably, it could
27 be hypothesized that the presence of an oxygen atom (aminoethoxy portion) switched the
28 ligand conformer towards the T99 side-chain, causing a slightly different docking mode
29 in comparison with that observed for T1AM.
30
31
32
33
34
35
36
37
38
39
40
41
42
43
44

45 **Conclusions**

46
47
48 Our efforts to identify potent and selective TAAR1 agonists synthetically more accessible
49 than traditional thyronamines led to the identification of a family of diphenyl methane
50 derivatives. By changing the biaryl-ether linkage present in thyronamines to a methylene
51 linkage we were able to use an efficient C-C bond forming reaction in the key biaryl-
52
53
54
55
56
57
58
59
60

1
2
3 coupling step. This process is amenable of extensive customization suggesting that a
4
5 great variety of thyronamine structural variants will be accessible through this synthetic
6
7 strategy. Analysis of the *in vitro* TAAR1 activity data reported herein showed that the
8
9 following structural modifications are well tolerated by *m*TAAR1: i) replacement of the
10
11 phenol hydroxyl with an amino group, ii) increase of the distance between the charged
12
13 amine and the aromatic ring by inserting an oxygen bridge, and iii) replacement of the 3-
14
15 iodo substituent with an alkyl group (i.e.CH₃). Compound **2** and **3** were found to be
16
17 approximately equipotent to T0AM and T1AM, respectively. When administered to mice
18
19 at a single dose of 1.32 µg/kg and 3.4 µg/kg both compounds increased plasma glycaemia
20
21 with a potency comparable to that of the corresponding parent compound. In addition, **2**
22
23 and **3** revealed to be both potent negative inotropic agents, with **3** being only slightly
24
25 more potent than **2**.
26
27
28
29
30
31

32 Experimental Section

33 Chemistry

34
35
36
37
38
39 **General material and methods.** Melting points were determined on a Kofler hot-stage
40
41 apparatus and are uncorrected. Chemical shifts (δ) are reported in parts per million
42
43 downfield from tetramethylsilane and referenced from solvent references; coupling
44
45 constants *J* are reported in hertz; ¹H NMR and ¹³C NMR spectra of all compounds were
46
47 obtained with a Varian Gemini 200 MHz or with a Bruker TopSpin 3.2 400 MHz
48
49 spectrometer. ¹³C NMR spectra were fully decoupled. The following abbreviations are
50
51 used: singlet (s), doublet (d), triplet (t), double-doublet (dd), and multiplet (m). The
52
53 elemental compositions of the compounds agreed to within \pm 0.4% of the calculated
54
55
56
57
58
59
60

1
2
3 values. Chromatographic separation was performed on silica gel columns by flash
4 (Kieselgel 40, 0.040–0.063 mm; Merck) or gravity column (Kieselgel 60, 0.063–0.200
5 mm; Merck) chromatography. The $\geq 95\%$ purity of the tested compounds was confirmed
6 by combustion analysis. Reactions were followed by thin-layer chromatography (TLC)
7 on Merck aluminum silica gel (60 F₂₅₄) sheets that were visualised under a UV lamp. The
8 microwave-assisted procedures were carried out with a CEM Discover LabMate
9 microwave. Evaporation was performed *in vacuo* (rotating evaporator). Sodium sulfate
10 was always used as the drying agent. Commercially available chemicals were purchased
11 from Sigma-Aldrich.

12
13
14
15
16
17
18
19
20
21
22
23
24
25 **4-(4-(2-Aminoethyl)benzyl)aniline (1)**. To a suspension of LiAlH₄ (405 mg; 3.04 mmol)
26 in THF was added dropwise a solution of AlCl₃ (405 mg; 3.04 mmol) in THF (200 mL),
27 and the mixture was stirred for 5 min at r.t. A solution of **14** (85.0 mg; 0.34 mmol) in
28 THF was added dropwise, and the mixture was heated at reflux for 12 h. The mixture was
29 cooled to 0°C with an ice bath and added dropwise with water and then with 10%
30 aqueous HCl. The mixture was extracted with diethyl ether, and the aqueous layer was
31 made alkaline with 2N aqueous NaOH and extracted with CHCl₃. The organic phase was
32 separated, washed with brine, dried, filtered, and concentrated. The crude product was
33 purified by conversion to the corresponding hydrochloride salt. White solid. mp: 165-
34 167°C. (70% yield). ¹H NMR (CD₃OD): δ 2.93 (t, 2H, *J* = 7.8 Hz; CH₂); 3.15 (t, 2H, *J* =
35 7.8 Hz; CH₂); 4.02 (s, 2H, CH₂); 7.25-7.20 (m, 4H, Ar); 7.33 (d, 2H, *J* = 8.4 Hz, Ar) 7.38
36 (d, 2H, *J* = 8.4 Hz, Ar) ppm. ¹³C NMR (CD₃OD): δ 142.83, 139.53, 134.58, 130.20,
37 129.12, 128.67, 128.50, 122.71, 40.54, 40.30, 32.75 ppm. Anal. (C₁₅H₁₈N₂) C, H, N. %
38 Calcd: 79.61 (C); 8.02 (H); 12.38 (N). % Found: 79.45 (C); 8.18 (H); 12.77 (N).
39
40
41
42
43
44
45
46
47
48
49
50
51
52
53
54
55
56
57
58
59
60

1
2
3
4
5
6 **4-(4-(2-Aminoethoxy)benzyl)aniline (2).** Compound **2** was synthesized from **17a** (96.3
7 mg; 0.34 mmol), LiAlH₄ (3.04 mmol) and AlCl₃ (405 mg; 3.04 mmol) in THF (200 mL)
8 following the same procedure described above for the preparation of **1**. The crude was
9 purified by conversion in the corresponding hydrochloride salt. White solid. mp: 137-
10 135°C. (70% yield). ¹H NMR (CD₃OD): δ 3.35 (t, 2H, *J* = 5.0 Hz; CH₂); 3.93 (s, 2H,
11 CH₂); 4.20 (t, 2H, *J* = 5.0 Hz; CH₂NH₂); 6.94 (d, 2H, *J* = 8.6 Hz, Ar); 7.16 (d, 2H, *J* =
12 8.3, Hz, Ar); 7.15 (d, 2H, *J* = 8.6 Hz, Ar); 7.26 (d, 2H, *J* = 8.3 Hz, Ar); ppm. ¹³C NMR
13 (CD₃OD): δ 158.13, 141.85, 135.52, 133.72, 131.24, 131.02, 122.40, 115.81, 65.32,
14 41.21, 40.39 ppm. Anal. (C₁₆H₂₁ClN₂O) C, H, N. % Calcd: 65.63 (C); 7.23 (H); 9.57 (N).
15
16
17
18
19
20
21
22
23
24
25
26
27
28
29
30
31
32
33
34
35
36
37
38
39
40
41
42
43
44
45
46
47
48
49
50
51
52
53
54
55
56
57
58
59
60
% Found: 65.61 (C); 7.52 (H); 9.73 (N).

30
31 **4-(4-(2-Aminoethoxy)-2-methylbenzyl)aniline (3).** Compound **3** was synthesized from
32 **17b** (101 mg; 0.34 mmol), LiAlH₄ (3.04 mmol) and AlCl₃ (405 mg; 3.04 mmol) in THF
33 (200 mL) following the same procedure described above for the preparation of **1**. The
34 crude was purified by conversion in the corresponding hydrochloride salt. White solid.
35 mp: 156-158°C. (75% yield). ¹H NMR (CD₃OD): δ 2.18 (s, 3H, CH₃); 3.36 (t, 2H, *J* = 4.0
36 Hz; CH₂); 4.00 (s, 2H, CH₂); 4.21 (t, 2H, *J* = 4.0 Hz; CH₂NH₂); 6.79-6.88 (m, 2H, Ar);
37 7.11 (d, 1H, *J* = 8.0 Hz, Ar); 7.28-7.34 (m, 4H, Ar) ppm. ¹³C NMR (CD₃OD): δ 158.32,
38 143.87, 139.32, 132.78, 132.22, 131.27, 129.71, 124.01, 117.86, 113.05, 65.23, 40.41,
39 38.89, 19.93 ppm. Anal. (C₁₅H₁₉ClN₂O) C, H, N. % Calcd: 64.63 (C); 6.87 (H); 10.05
40
41
42
43
44
45
46
47
48
49
50
51
52
53
54
55
56
57
58
59
60
(N). % Found: 64.74 (C); 7.02 (H); 9.95 (N).

54
55 **4-(4-(2-Aminoethoxy)benzyl)phenol (4).**

1
2
3
4
5
6
7
8
9
10
11
12
13
14
15
16
17
18
19
20
21
22
23
24
25
26
27
28
29
30
31
32
33
34
35
36
37
38
39
40
41
42
43
44
45
46
47
48
49
50
51
52
53
54
55
56
57
58
59
60

Compound **4** was synthesized from **20a** (32.3 mg; 0.13 mmol), LiAlH₄ (1.21 mmol) and AlCl₃ (161 mg; 1.21 mmol) in THF (200 mL) following the same procedure described above for the preparation of **1**. The crude product was purified by conversion to the corresponding hydrochloride salt. White solid. mp: 175-177°C. (50% yield). ¹H NMR (CD₃OD): δ 3.34 (t, 2H, *J* = 4.8 Hz; CH₂); 3.80 (s, 2H, CH₂); 4.20 (t, 2H, *J* = 4.8 Hz; CH₂NH₂); 6.68 (d, 2H, *J* = 8.4 Hz, Ar); 6.91 (d, 2H, *J* = 8.8 Hz, Ar); 6.97 (d, 2H, *J* = 8.4 Hz, Ar); 7.11 (d, 2H, *J* = 8.8 Hz Ar) ppm. ¹³C NMR (CD₃OD): δ 156.62, 136.83, 133.80, 130.88, 130.71, 116.15, 115.61, 65.30, 41.07, 40.40 ppm Anal. (C₁₅H₁₇NO₂) C, H, N. % Calcd: 74.05 (C); 7.04 (H); 5.76 (N). % Found: 74.31 (C); 7.22 (H); 5.73 (N).

2-(4-(4-Aminobenzyl)phenyl)acetic acid (5). To a solution of **6** (167 mg; 0.64 mmol) in MeOH (50 mL) was added carbon (33.7 mg) and FeCl₃ (7 mg). The reaction mixture was warmed to 60 °C, then hydrazine monohydrate was added dropwise (0.33 mL, 6.71 mmol). The mixture was refluxed overnight then filtered on a celite pad, and the solvent removed. The residue was dissolved in AcOEt and washed with water. The organic layer was dried and evaporated under reduced pressure. The crude was purified by conversion in the corresponding hydrochloride salt. White solid. Mp: 154-156°C. (72% yield). ¹H NMR (CD₃OD): δ 3.61 (s, 2H, CH₂); 4.01 (s, 2H, CH₂); 7.19 (d, 2H, *J* = 8.0 Hz, Ar); 7.26 (d, 2H, *J* = 8.0 Hz, Ar); 7.31 (d, 2H, *J* = 8.4 Hz, Ar); 7.37 (d, 2H, *J* = 8.4 Hz, Ar) ppm. ¹³C NMR (CD₃OD): δ 175.61, 144.37, 144.32, 140.46, 134.15, 131.60, 130.65, 130.60, 130.03, 129.98, 129.80, 129.37, 124.04, 41.69, 41.42 ppm. Anal. (C₁₅H₁₃NO₄·HCl) C, H, N. % Calcd: 64.87 (C); 5.81 (H); 5.04 (N). % Found: 64.72 (C); 5.92 (H); 5.09 (N).

1
2
3
4
5
6
7
8
9
10
11
12
13
14
15
16
17
18
19
20
21
22
23
24
25
26
27
28
29
30
31
32
33
34
35
36
37
38
39
40
41
42
43
44
45
46
47
48
49
50
51
52
53
54
55
56
57
58
59
60

2-(4-(4-Nitrobenzyl)phenyl)acetic acid (6). A solution of **14** (51.6 mg, 0.20 mmol) in 50% H₂SO₄ (0.2 ml) was placed under stirring at reflux for 30 min. After cooling, the water was added, and the solid precipitate was collected to give **6**. Yellow solid. mp: 175-177°C. (79% yield). ¹H NMR (CDCl₃): δ 3.58 (s, 2H, CH₂); 4.09 (s, 2H, CH₂); 7.19 (d, 2H, *J* = 7.6 Hz, Ar); 7.37-7.27 (m, 4H, Ar); 8.17 (d, 2H, *J* = 7.6 Hz, Ar) ppm. ¹³C NMR (CDCl₃): δ 173.69, 148.41, 146.52, 138.46, 133.08, 129.77, 129.59, 129.51, 129.08, 123.75, 123.69, 42.65, 41.25 ppm. Anal. (C₁₅H₁₃NO₄) C, H, N. % Calcd: 66.41 (C); 4.83 (H); 5.16 (N). % Found: 66.44 (C); 4.55 (H); 5.28 (N).

2-(4-(4-Aminobenzyl)phenoxy)acetic acid (7). Compound **7** was synthesized from **8** (184.0 mg; 0.64 mmol), hydrazine monohydrate (6.71 mmol), carbon (33.7 mg) and FeCl₃ (7 mg) in MeOH (50 mL) following the same procedure described above for the preparation of **5**. The residue was dissolved in AcOEt and washed with water. The organic layer was dried and evaporated under reduced pressure. White solid. Mp: 153-155°C. (70% yield). ¹H NMR (CDCl₃): δ 3.82 (s, 2H, CH₂); 4.54 (s, 2H, CH₂); 6.62 (d, 2H, *J* = 8.4 Hz, Ar); 6.81 (d, 2H, *J* = 8.4 Hz, Ar); 6.95 (d, 2H, *J* = 8.4 Hz, Ar); 7.11 (d, 2H, *J* = 8.4 Hz, Ar) ppm. ¹³C NMR (CDCl₃): δ 168.76, 155.34, 144.52, 135.92, 131.22, 130.04, 129.65, 115.34, 114.49, 67.09, 40.14 ppm. Anal. (C₁₅H₁₅NO₃) C, H, N. % Calcd: 70.02 (C); 5.88 (H); 5.44 (N). % Found: 70.39 (C); 5.93 (H); 5.59 (N).

2-(4-(4-Nitrobenzyl)phenoxy)acetic acid (8). To a solution of the ester **18a** (179.7 mg; 0.57 mmol) in MeOH was added dropwise an aqueous solution of NaOH 10% (0.2 mL); the resulting solution was refluxed for 30min., then, after cooling, the solvent was evaporated. The residue was acidified to pH 3 with HCl 1N and the precipitate was filtered off, washed with H₂O, and dried. White solid. Mp: 162-164°C. (87% yield). ¹H

1
2
3 NMR (CDCl₃): δ 4.02 (s, 2H, CH₂); 4.66 (s, 2H, CH₂); 6.88 (d, 2H, *J* = 8.4 Hz, Ar); 7.11
4
5 (d, 2H, *J* = 8.4 Hz, Ar); 7.31 (d, 2H, *J* = 8.4 Hz, Ar); 8.14 (d, 2H, *J* = 8.4 Hz Ar) ppm.
6
7 ¹³C NMR (200MHz, CDCl₃) δ: 158.60; 146.30; 130.22; 129.56; 128.00; 123.79; 123.15;
8
9 115.03; 77.35; 64.89; 29.70 ppm Anal. (C₁₅H₁₃NO₅) C, H, N. % Calcd: 62.72 (C); 4.56
10
11 (H); 4.88 (N). % Found: 62.91 (C); 4.23 (H); 4.59 (N).
12
13
14
15

16 **2-(4-(4-Aminobenzyl)-3-methylphenoxy)acetic acid (9)**. Compound **9** was synthesized
17
18 from **10** (192.8 mg; 0.64 mmol), hydrazine monohydrate (6.71 mmol), carbon (33.7 mg)
19
20 and FeCl₃ (7 mg) in MeOH (50 mL) following the same procedure described above for
21
22 the preparation of **5**. The residue was dissolved in AcOEt and washed with water. The
23
24 organic layer was dried and evaporated under reduced pressure. The crude was purified
25
26 by conversion in the corresponding hydrochloride salt. White solid. mp: 175-177°C.
27
28 (65% yield). ¹H NMR (CD₃OD): δ 2.16 (s, 3H, CH₃); 3.77 (s, 2H, CH₂); 4.36 (s, 2H,
29
30 CH₂); 6.57-6.80 (m, 4H, Ar); 6.81-6.89 (m, 2H, Ar) 6.92-7.01 (m, 2H, Ar) ppm. Anal.
31
32 (C₁₆H₁₇NO₃) C, H, N. % Calc. 70.83 (C); 6.32 (H); 5.16 (N). % Found. 70.90 (C); 6.37
33
34 (H); 5.29 (N).
35
36
37
38
39

40 **2-(3-Methyl-4-(4-nitrobenzyl)phenoxy)acetic acid (10)**. Compound **10** was synthesized
41
42 from **18b** (187.7 mg; 0.57 mmol) and an aqueous solution of NaOH 10% (0.2 mL) in
43
44 MeOH following the same procedure described above for the preparation of **8**. The
45
46 residue was acidified to pH 3 with HCl 1N and the precipitate was filtered off, washed
47
48 with H₂O, and dried. White solid. Mp: 166-168°C. (90% yield). ¹H NMR (CDCl₃): δ 2.17
49
50 (s, 3H, CH₃), 4.02 (s, 2H, CH₂); 4.68 (s, 2H, CH₂); 6.70-6.80 (m, 2H, Ar); 7.03 (d, 1H, *J*
51
52 = 8.2 Hz, Ar); 7.24 (d, 2H, *J* = 7.9 Hz, Ar); 8.12 (d, 2H, *J* = 7.9 Hz, Ar) ppm. ¹³C NMR
53
54 (CDCl₃) δ: 156.46; 148.56; 138.54; 131.33; 131.10; 130.88; 129.42; 123.84; 117.27;
55
56
57
58
59
60

1
2
3 112.04; 77.80; 64.93; 38.73; 20.06 ppm Anal. (C₁₆H₁₅NO₅) C, H, N. % Calcd: 63.78 (C);
4
5 5.02 (H); 4.65 (N). % Found: 63.87 (C); 5.21 (H); 4.51 (N).
6
7

8
9 **Potassium trifluoro(4-(hydroxymethyl)phenyl)borate (11)**. To a round-bottomed flask
10 containing the 4-(hydroxymethyl)phenylboronic acid (1.3 g; 8.55 mmol) in MeOH was
11 added a solution of KHF₂ (2.7 g; 34.2 mmol) in distilled water at 0°C. The mixture was
12 stirred for 2h, at rt, and then the solvent was completely removed under reduced pressure.
13
14 The crude product was purified by crystallization from iPrOH to give **11**. White solid.
15
16 (63% yield). ¹H NMR (CD₃OD): δ 4.53 (s, 2H, CH₂); 7.18 (d, 2H, *J* = 7.2 Hz, Ar); 7.48
17
18 (d, 2H, *J* = 7.2 Hz, Ar) ppm. Anal. (C₇H₇BF₃KO) C, H, N. % Calcd: 39.28 (C); 3.30 (H).
19
20 % Found: 39.55 (C); 3.43 (H).
21
22
23
24
25
26
27

28
29 **(4-(4-Nitrobenzyl)phenyl)methanol (12)**. To a solution of trifluoroborane salt **11** (509
30 mg; 2.38 mmol) in dioxane/H₂O 9:1 (4 mL) was added, under nitrogen atmosphere, *p*-
31 nitrobenzyl bromide (513 mg; 2.38 mmol), cesium carbonate (2.30 g; 7.1 mmol) and
32 PdCl₂dppf (34.8 mg; 0.05 mmol). The resulting mixture was stirred at 95°C for 24 h in a
33 sealed vial. The crude mixture was evaporated and then diluted with water and extracted
34 with DCM. The organic phase was dried over sodium sulfate and the solvent removed.
35
36 The crude product was chromatographed on a silica gel column, eluting with *n*-
37 hexane/AcOEt (70:30). White oil. (32% yield). ¹H NMR (CDCl₃): δ 4.08 (s, 2H, CH₂);
38
39 4.68 (s, 2H, CH₂OH); 7.17 (d, 2H, *J* = 8.0 Hz Ar); 7.34-7.32 (m, 4H, Ar); 8.14 (d, 2H, *J*=
40
41 8.4 Hz, Ar) ppm. Anal. (C₁₄H₁₃NO₃) C, H, N. % Calcd: 69.12 (C); 5.39 (H); 5.76 (N). %
42
43 Found: 69.03 (C); 5.63 (H); 5.58 (N).
44
45
46
47
48
49
50
51
52
53
54
55
56
57
58
59
60

1
2
3 **1-(Chloromethyl)-4-(4-nitrobenzyl)benzene (13)**. To a solution of **12** (86.4 mg; 0.35
4 mmoli) in CHCl_3 at 0°C was added SOCl_2 (3.50 mmol; 0.25 mL). The reaction mixture
5
6 was stirred for 2h at room temperature, then, the solvent was evaporated. The residue was
7
8 dissolved in H_2O and alkalized with NaOH 1N; and the aqueous layer was extracted with
9
10 DCM. The organic phase was dried and the solvent was evaporated to give **13**, which was
11
12 used without further purification. Yellow oil. (83% yield). ^1H NMR (CDCl_3): δ 4.08 (s,
13 2H, CH_2); 4.57 (s, 2H, CH_2); 7.17 (d, 2H, $J = 8.0$ Hz, Ar); 7.35-7.32 (m, 4H, Ar); 8.15 (d,
14 2H, $J = 8.8$ Hz Ar) ppm. Anal. ($\text{C}_{14}\text{H}_{12}\text{ClNO}_2$) C, H, N. % Calcd: 64.25 (C); 4.62 (H);
15 5.35 (N). % Found: 63.96 (C); 4.46 (H); 5.71 (N).
16
17
18
19
20
21
22
23

24
25 **2-(4-(4-Nitrobenzyl)phenyl)acetonitrile (14)**. To a solution of **13** (152 mg; 0.58 mmol)
26 in CH_3CN (0.78ml) was added NaCN (57.0 mg; 1.16 mmol) in H_2O (0.26 ml). The
27 mixture was submitted to microwave irradiation (150W, 100°C , 20 min). After cooling
28 the solution was extracted with DCM. Organic phase was dried and evaporated to
29 dryness. Yellow oil. (86% yield). ^1H NMR (CDCl_3): δ 3.73 (s, 2H, CH_2), 4.08 (s, 2H,
30 CH_2); 7.19 (d, 2H, $J = 8.0$ Hz; Ar); 7.33-7.28 (m, 4H, Ar); 8.15 (d, 2H, $J = 8.8$ Hz; Ar)
31 ppm. Anal. ($\text{C}_{15}\text{H}_{12}\text{N}_2\text{O}_2$) C, H, N. % Calcd: 71.42 (C); 4.79 (H); 11.10 (N). % Found:
32 71.56 (C); 4.64 (H); 11.33 (N).
33
34
35
36
37
38
39
40
41
42
43
44

45 **General procedure for synthesis of compounds 15a,b**

46
47
48 To a solution of arylboronic acid (2.63mmoli) in acetone/ H_2O 1:1 (4 mL) was added,
49 under nitrogen flux, p-nitrobenzyl bromide (569 mg, 2.63 mmol), K_2CO_3 (1.24 g,
50 6.58 mmol) and a catalytic amount of PdCl_2 . The resulting mixture was stirred at r.t. for
51
52 62 h in a sealed vial. The crude mixture was evaporated and then diluted with water and
53
54
55
56
57
58
59
60

1
2
3 extracted with Et₂O. The organic phase was dried over sodium sulfate and concentrated
4
5 under vacuum.
6

7
8
9 **1-Methoxy-4-(4-nitrobenzyl)benzene (15a)**. The crude residue was purified by column
10 chromatography *n*-hexane/AcOEt (97:3), affording **15a** (47% yield). Yellow oil. ¹H
11 NMR (CDCl₃): δ 3.79 (s, 3H, OCH₃); 4.02 (s, 2H, CH₂); 6.86 (d, 2H, *J* = 8.3 Hz, Ar);
12
13 7.10 (d, 2H, *J* = 8.3 Hz, Ar); 7.32 (d, 2H, *J*=8.3 Hz, Ar); 8.13 (d, 2H, *J*=8.3 Hz, Ar) ppm.
14
15 Anal. (C₁₄H₁₃NO₃) C, H, N. % Calcd: 69.12 (C); 5.39 (H); 5.76 (N). % Found: 69.21 (C);
16
17 5.43 (H); 5.98 (N).
18
19
20
21
22

23
24 **4-Methoxy-2-methyl-1-(4-nitrobenzyl)benzene (15b)**. The crude residue was purified
25 by column chromatography *n*-hexane/AcOEt (97:3), affording **15b** (49% yield). Yellow
26 oil. ¹H NMR (CDCl₃): δ 2.15 (s, 3H, CH₃); 3.78 (s, 3H, OCH₃); 4.01 (s, 2H, CH₂); 6.69-
27
28 6.80 (m, 2H, Ar); 7.01 (s, 1H, Ar); 7.23 (d, 2H, *J* = 8.4 Hz, Ar); 8.10 (d, 2H, *J* = 8.4 Hz,
29
30 Ar) ppm. Anal. (C₁₅H₁₅NO₃) C, H, N. % Calcd: 70.02 (C); 5.88 (H); 5.44 (N). % Found:
31
32 70.22 (C); 5.93 (H); 5.62 (N).
33
34
35
36
37

38 39 **General procedure for synthesis of compounds 16a,b**

40
41
42 A solution of **15a,b** (0.39 mmol) in anhydrous DCM (1.5 mL) was cooled to -78 °C and
43 treated dropwise with a solution of BBr₃ in DCM (3.94 mL, 1.24 mmol); the resulting
44 solution was stirred at the same temperature for 5 min and at 0 °C for 1 h. The mixture
45 was then diluted with water and extracted with DCM. Organic phase was dried and
46 evaporated to give the products **16a** or **16b**.
47
48
49
50
51
52

53
54
55 **4-(4-Nitrobenzyl)phenol (16a)**. White oil. (95% yield). ¹H NMR (CDCl₃): δ 4.00 (s, 2H,
56 CH₂); 6.78 (d, 2H, *J* = 7.5 Hz, Ar); 7.04 (d, 2H, *J* = 7.5 Hz, Ar) 7.32 (d, 2H, *J* = 7.9 Hz,
57
58
59
60

Ar); 8.14 (d, 2H, $J=7.9$ Hz, Ar) ppm. Anal. ($C_{13}H_{11}NO_3$) C, H, N. % Calcd: 68.11 (C); 4.84 (H); 6.11 (N). % Found: 68.29 (C); 4.96 (H); 6.29 (N).

3-Methyl-4-(4-nitrobenzyl)phenol (16b). Pale yellow oil. (64% yield). 1H NMR ($CDCl_3$): δ 2.13 (s, 3H, CH_3); 4.00 (s, 2H, CH_2); 6.65-6.59 (m, 2H, Ar); 6.96 (s, 1H, Ar); 7.24 (d, 2H, $J=7.9$ Hz, Ar); 8.11 (d, 2H, $J=7.9$ Hz, Ar) ppm. Anal. ($C_{14}H_{13}NO_3$) C, H, N. % Calcd: 69.12 (C); 5.39 (H); 5.76 (N). % Found: 69.33 (C); 5.51 (H); 5.82 (N).

General procedure for synthesis of compounds 17a,b

To a mixture of cesium carbonate (725 mg, 2.22 mmol) and phenol **16a,b** (0.44 mmol) in 50mL of DMF was added $BrCH_2CN$ (0.03 mL, 0.44 mmol). The reaction mixture was stirred for 30 min at r.t., poured into 100mL of cold HCl 1N, and extracted with AcOEt. The organic phase was dried and evaporated.

2-(4-(4-Nitrobenzyl)phenoxy)acetonitrile (17a). The crude product was purified by chromatography eluting with *n*-hexane/AcOEt (70:30). White oil. (96% yield). 1H NMR ($CDCl_3$): δ 4.05 (s, 2H, CH_2); 4.76 (s, 2H, CH_2); 6.94 (d, 2H, $J = 8.6$ Hz, Ar); 7.15 (d, 2H, $J = 8.6$ Hz, Ar) 7.31 (d, 2H, $J=8.6$ Hz, Ar); 8.14 (d, 2H, $J=8.6$ Hz, Ar) ppm. Anal. ($C_{15}H_{12}N_2O_3$) C, H, N. % Calcd: 67.16 (C); 4.51 (H); 10.44 (N). % Found: 67.24 (C); 4.72 (H); 10.62 (N).

2-(3-Methyl-4-(4-nitrobenzyl)phenoxy)acetonitrile (17b). The crude product was purified by chromatography eluting with *n*-hexane/AcOEt (70:30). White oil. (98% yield). 1H NMR ($CDCl_3$): δ 2.19 (s, 3H, CH_3); 4.03 (s, 2H, CH_2); 4.76 (s, 2H, CH_2); 6.81-6.77 (m, 2H, Ar); 7.08 (s, 1H, Ar); 7.25 (d, 2H, $J = 8.6$ Hz, Ar); 8.13 (d, 2H, $J = 8.6$ Hz,

Ar) ppm. Anal. (C₁₆H₁₄N₂O₃) C, H, N. % Calcd: 68.07 (C); 5.00 (H); 9.92 (N). % Found: 68.21 (C); 5.11 (H); 9.86 (N).

General procedure for synthesis of compounds 18a,b

Compound 18a,b was synthesized from 16a,b (0.44 mmol) and BrCH₂COOEt (73.5mg, 0.44 mmol) in DMF (1.2 mL) following the same procedure as described above for the preparation of 17a,b

Ethyl 2-(4-(4-nitrobenzyl)phenoxy)acetate (18a). Yellow oil. (83% yield). ¹H NMR (CDCl₃): δ 1.27 (t, 3H, *J*=7.1Hz, CH₃); 4.02 (s, 2H, CH₂); 4.27 (q, 2H, *J*=7.1Hz, CH₂); 4.60 (s, 2H, CH₂); 6.86 (d, 2H, *J* = 8.4 Hz); 7.09 (d, 2H, *J* = 8.8 Hz); 7.31 (d, 2H, *J* = 8.8 Hz); 8.13 (d, 2H, *J* = 8.4 Hz) ppm. Anal. (C₁₇H₁₇NO₅) C, H, N. % Calcd: 64.75 (C); 5.43 (H); 4.44 (N). % Found: 64.80 (C); 5.71 (H); 4.69 (N).

Ethyl 2-(3-methyl-4-(4-nitrobenzyl)phenoxy)acetate (18b). Yellow oil. (60% yield). ¹H NMR (CDCl₃): δ 1.26 (t, 3H, *J*=7.0 Hz, CH₃); 2.12 (s, 3H, CH₃); 3.98 (s, 2H, CH₂); 4.23 (q, 2H, *J*=7.0 Hz, CH₂); 4.57 (s, 2H, CH₂); 6.32-6.79 (m, 2H, Ar); 6.97 (d, 1H, *J* = 8.2 Hz, Ar) 7.21 (d, 2H, *J* =8.5 Hz, Ar); 8.08 (d, 2H, *J* = 8.5 Hz, Ar) ppm. Anal. (C₁₈H₁₉NO₅) C, H, N. % Calcd: 65.64 (C); 5.81 (H); 4.25 (N). % Found: 65.91 (C); 5.93 (H); 4.39 (N).

2-(4-(4-Aminobenzyl)phenoxy)acetonitrile (19a). A solution of 17a (136 mg, 0.5 mmoli) in AcOH (10 mL) was hydrogenated in the presence of 10% Pd-C (28.3 mg), for 12 h. Then the catalyst was filtered off, and the solvent was removed to dryness to give a crude product that was used in the subsequent step without any further purification. Yellow oil. (52% yield). ¹H NMR (CDCl₃) δ: 3.83 (s, 2H, CH₂); 4.73 (s, 2H, CH₂CN);

1
2
3 6.63 (d, 2H, $J = 8.4$ Hz, Ar); 6.89 (d, 2H, $J = 8.4$ Hz, Ar); 6.95 (d, 2H, $J = 8.4$ Hz, Ar);
4
5 7.14 (d, 2H, $J = 8.4$ Hz, Ar) ppm. Anal. ($C_{15}H_{14}N_2O$) C, H, N. % Calcd: 75.61 (C); 5.92
6
7 (H); 11.76 (N). % Found: 75.70 (C); 6.07 (H); 11.61 (N).
8
9

10
11 **2-(4-(4-Hydroxybenzyl)phenoxy)acetonitrile (20a)**. To a mixture of aniline derivative
12
13 **19a** (63.0 mg, 0.26 mmol) in H_2O was added dropwise with H_2SO_{4conc} (0.06 mL) and the
14
15 mixture was stirred at room temperature for 20 min. Then a solution $NaNO_2$ (17.9 mg,
16
17 0.26 mmol) in H_2O (0.19 mL) was added dropwise to the reaction mixture. The resulting
18
19 solution was stirred for 1 h at $100^\circ C$. The mixture was cooled to room temperature, and
20
21 the residue diluted with AcOEt and washed with brine. The collected organic layers were
22
23 dried and evaporated to give compound **20a** that was directly used in the next step. White
24
25 solid. mp: $151-153^\circ C$. (61% yield). 1H NMR ($CDCl_3$) δ : 3.87 (s, 2H, CH_2); 4.74 (s, 2H,
26
27 CH_2CN); 6.76 (d, 2H, $J = 8.4$ Hz, Ar); 6.90 (d, 2H, $J = 8.4$ Hz, Ar); 7.02 (d, 2H, $J = 8.4$
28
29 Hz, Ar); 7.14 (d, 2H, $J = 8.4$ Hz, Ar) ppm. Anal. ($C_{15}H_{13}NO_2$) C, H, N. % Calcd: 75.30
30
31 (C); 5.48 (H); 5.85 (N). % Found: 74.92 (C); 5.48 (H); 6.13 (N).
32
33
34
35
36
37

38 **Molecular Modeling**

39
40
41 ***mTAAR1* Homology Modeling**. In absence of crystallographic data for the TAAR1
42
43 receptor, we built a theoretical model of the *mTAAR1*, and then used for docking
44
45 simulations. Since most of the key residues characteristic of GPCRs are conserved in
46
47 TAAR1 receptor, a *mTAAR1* receptor homology model was generated, starting from the
48
49 X-ray structure of human β_2 -adrenoreceptor (PDB code: 3PDS; resolution = 3.50 \AA), in
50
51 complex with an agonist compound³⁵. The amino acid sequence of *mTAAR1* (Q923Y8)
52
53
54
55
56
57
58
59
60

1
2
3 was retrieved from the SWISSPROT database³⁶ while the three-dimensional structure co-
4
5
6 ordinates file of the GPCR template was obtained from the Protein Data Bank³⁷.
7

8
9 The amino acid sequences of *m*TAAR1 TM helices were aligned with the corresponding
10
11 residues of 3PDS, on the basis of the Blosum62 matrix (MOE software). The connecting
12
13 loops were constructed by the loop search method implemented in MOE. The MOE
14
15 output file included a series of ten *h*TAAR1 models which were independently built on
16
17 the basis of a Boltzmann-weighted randomized procedure³⁸, combined with specialized
18
19 logic for the handling of sequence insertions and deletions³⁹. Among the derived models,
20
21 there were no significant main chain deviations. The model with the best packing quality
22
23 function was selected for full energy minimization. The retained structure was minimized
24
25 with MOE using the AMBER94 force field⁴⁰. The energy minimization was carried out
26
27 by the 1000 steps of steepest descent followed by conjugate gradient minimization until
28
29 the rms gradient of the potential energy was less than 0.1 kcal mol⁻¹ Å⁻¹. The assessment
30
31 of the final obtained model was performed using Ramachandran plots, generated within
32
33 MOE.
34
35
36
37
38

39
40 Following the same procedure already described by us³⁴, the putative receptor model
41
42 binding site was identified on the basis of the corresponding regions of the 3PDS binding
43
44 site, and also by taking into account the recent mutagenesis data published by Grandy
45
46 D.K⁴¹.
47
48

50 51 **Ligand preparation**

52
53 All compounds were built, parameterised (Gasteiger-Huckel method) and energy
54
55 minimised within MOE using MMFF94 forcefield [MOE: Chemical Computing Group
56
57
58
59
60

1
2
3 Inc. Montreal. H3A2R7 Canada. <http://www.chemcomp.comp>]. For all compounds, the
4
5 protonated form was considered for the *in silico* analyses.
6
7

8 9 **Docking studies**

10
11 Docking studies were subsequently performed, according to the following protocol. Each
12
13 isomer was docked into the putative ligand binding site by means of the Surflex docking
14
15 module implemented in Sybyl-X1.0. Then, for all the compounds, the best docking
16
17 geometries (selected on the basis of the SurFlex scoring functions) were refined by
18
19 ligand/receptor complex energy minimization (CHARMM27) by means of the MOE
20
21 software. To verify the reliability of the derived docking poses, the obtained
22
23 ligand/receptor complexes were further investigated by docking calculations (10 run),
24
25 using MOE-Dock (Genetic algorithm; applied on the poses already located into the
26
27 putative TAAR1 receptor). The conformers showing lower energy scoring functions and
28
29 rmsd values (respect to the starting poses) were selected as the most stable and allowed
30
31 us to identify the most probable conformers interacting with *mTAAR1*.
32
33
34
35
36
37
38

39 **In vitro biological studies**

40 41 42 **Bioluminescence Resonance Energy Transfer (BRET) measurement**

43
44
45 HEK-293 cells were transiently transfected with *mTAAR1* and a cAMP BRET biosensor
46
47 (EPAC) and then plated in a 96-well plate as described³⁰. For time course experiments,
48
49 the plate was read immediately after the addition of the agonist and for approximately 20
50
51 minutes. All the compounds were tested at the initial concentration of 10 μ M. Then, for
52
53 active compounds, a dose response was performed, in order to calculate the EC₅₀ values.
54
55
56
57 All the experiments were conducted in presence of the phosphodiesterase inhibitor IBMX
58
59
60

1
2
3 (Sigma) at the final concentration of 200 μ M. Readings were collected using a Tecan
4
5 Infinite instrument that allows the sequential integration of the signals detected in the 465
6
7 to 505nm and 515 to 555 nm windows using filters with the appropriate band pass and by
8
9 using iControl software. The acceptor/donor ratio was calculated as previously
10
11 described⁴². Curve was fitted using a nonlinear regression and one site specific binding
12
13 with GraphPad Prism 5. Data are representative of 4-6 independent experiments and are
14
15 expressed as means \pm SEM.
16
17
18
19

20 21 **Cardiac perfusion technique**

22
23
24 Male Wistar rats (275–300 g body wt), fed with standard diet, were anesthetized with a
25
26 mixture of ether and air. After injection of 1000 U sodium heparin in the femoral vein,
27
28 the heart was quickly excised and perfused according to the working heart technique, as
29
30 described previously⁴³. The height of the atrial and aortic cannulae was set at 20 and 100
31
32 cm, respectively. Unless otherwise specified, the perfusion buffer included (mM): 118
33
34 NaCl, 25 NaHCO₃, 4.5 KCl, 1.2 KH₂PO₄, 1.2 MgSO₄, 1.5 CaCl₂, and 11 glucose.
35
36 Perfusions were carried out using 200 ml of recirculating buffer, which was equilibrated
37
38 with a mixture of O₂ (95%) and CO₂ (5%). Temperature was kept between 36.8 and
39
40 37°C, and the pH was 7.4.
41
42
43
44

45
46 After an equilibration period of 5 min, hearts were perfused for 60 min: 100 μ l of DMSO
47
48 (vehicle) or increasing doses of **2** and **3** dissolved in DMSO were added to the standard
49
50 perfusion buffer. Aortic pressure and heart rate were continuously recorded on a personal
51
52 computer. Cardiac output was determined as the sum of aortic and coronary flow.
53
54 Powerlab/200 (ADInstruments, Castle Hill, Australia) was used for data acquisition.
55
56
57
58
59
60

Measurement of plasma glycaemia

Glycaemia was monitored in blood collected from the tail vein of 4 h (from 8h to 12h) fasted mice (male, CD-1 strain), who had received T0AM, T1AM, **2** and **3** (1.32, 4 and 11 $\mu\text{g}\cdot\text{kg}^{-1}$ i.p.) or saline (i.p.) ($n = 10$ in each group). Glycaemia was evaluated by a glucrefractometer 15 min after the i.p. injections, as described²⁰. Data are expressed as mean \pm SEM of independent experiments. Statistical analysis was performed by one-way ANOVA, followed by Student–Newman–Keuls multiple comparison post hoc test; the threshold of statistical significance was set at $P < 0.05$. Data analysis was performed by GraphPad Prism 5.0 statistical program (GraphPad software, San Diego, CA, USA).

AUTHOR INFORMATION

Corresponding Author

*Grazia Chiellini. E-mail: g.chiellini@bm.med.unipi.it; Phone: +39 050 2218677

*Simona Rapposelli. E-mail: simona.rapposelli@farm.unipi.it ; Phone: +39 050 2219582.

Notes

The authors declare no competing financial interest

ABBREVIATION USED

T1AM, 3-iodothyronamine; T0AM, thyronamine; β -PEA, β -phenylethylamine; TA0, thyroacetic acid; TA1, 3-iodothyroacetic acid;

ACKNOWLEDGEMENTS

We thank Prof. Scanlan from the University of Oregon (USA) for supplying us T1AM, T0AM. This work was supported by a local grant from the University of Pisa (to GC, RZ and SR). BRET studies has been supported by the Russian Science Foundation grant N14-25-00065 (to RRG).

References

1. Scanlan, T. S.; Suchland, K. L.; Hart, M. E.; Chiellini, G.; Huang, Y.; Kruzich, P. J.; Frascarelli, S.; Crossley, D. A.; Bunzow, J. R.; Ronca-Testoni, S., 3-Iodothyronamine is an endogenous and rapid-acting derivative of thyroid hormone. *Nat. Med.* **2004**, *10*, 638-642.
2. Saba, A.; Chiellini, G.; Frascarelli, S.; Marchini, M.; Ghelardoni, S.; Raffaelli, A.; Tonacchera, M.; Vitti, P.; Scanlan, T. S.; Zucchi, R., Tissue distribution and cardiac metabolism of 3-iodothyronamine. *Endocrinology* **2010**, *151*, 5063-5073.
3. Hoefig, C. S.; Köhrle, J.; Brabant, G.; Dixit, K.; Yap, B.; Strasburger, C. J.; Wu, Z., Evidence for extrathyroidal formation of 3-iodothyronamine in humans as provided by a novel monoclonal antibody-based chemiluminescent serum immunoassay. *J. Clin. Endocrinol. Metab.* **2011**, *96*, 1864-1872.
4. Hackenmueller, S. A.; Marchini, M.; Saba, A.; Zucchi, R.; Scanlan, T. S., Biosynthesis of 3-iodothyronamine (T1AM) is dependent on the sodium-iodide symporter and thyroperoxidase but does not involve extrathyroidal metabolism of T4. *Endocrinology* **2012**, *153*, 5659-5667.
5. Höfig, C. W. T., Lehmphul I, Daniel H, Schweizer U, Mittag J, Köhrle J. Biosynthesis of 3-iodothyronamine from thyroxine in intestinal tissue, *Eur. Thyroid J.* **2014**, 3(Supp. 1), 98-99.

- 1
2
3
4
5
6
7
8
9
10
11
12
13
14
15
16
17
18
19
20
21
22
23
24
25
26
27
28
29
30
31
32
33
34
35
36
37
38
39
40
41
42
43
44
45
46
47
48
49
50
51
52
53
54
55
56
57
58
59
60
6. Revel, F.; Moreau, J.; Pouzet, B.; Mory, R.; Bradaia, A.; Buchy, D.; Metzler, V.; Chaboz, S.; Zbinden, K. G.; Galley, G., A new perspective for schizophrenia: TAAR1 agonists reveal antipsychotic-and antidepressant-like activity, improve cognition and control body weight. *Mol. Psychiatry* **2013**, *18*, 543-556.
7. Espinoza, S.; Gainetdinov, R. R., Neuronal functions and emerging pharmacology of TAAR1. In *Topics in Medicinal Chemistry*, Springer Berlin Heidelberg: Berlin, **2014**; pp.1-20
8. Bunzow, J. R.; Sonders, M. S.; Arttamangkul, S.; Harrison, L. M.; Zhang, G.; Quigley, D. I.; Darland, T.; Suchland, K. L.; Pasumamula, S.; Kennedy, J. L., Amphetamine, 3, 4-methylenedioxymethamphetamine, lysergic acid diethylamide, and metabolites of the catecholamine neurotransmitters are agonists of a rat trace amine receptor. *Mol. Pharm.* **2001**, *60*, 1181-1188.
9. Borowsky, B.; Adham, N.; Jones, K. A.; Raddatz, R.; Artymyshyn, R.; Ogozalek, K. L.; Durkin, M. M.; Lakhani, P. P.; Bonini, J. A.; Pathirana, S., Trace amines: identification of a family of mammalian G protein-coupled receptors. *PNAS* **2001**, *98*, 8966-8971.
10. Lindemann, L.; Meyer, C. A.; Jeanneau, K.; Bradaia, A.; Ozmen, L.; Bluethmann, H.; Bettler, B.; Wettstein, J. G.; Borroni, E.; Moreau, J.-L., Trace amine-associated receptor 1 modulates dopaminergic activity. *J. Pharm. Exp. Ther.* **2008**, *324*, 948-956.
11. Roy, G.; Placzek, E.; Scanlan, T.S.; ApoB-100-containing Lipoproteins Are Major Carriers of 3-Iodothyronamine in Circulation. *J. Biol. Chem.* **2012**, *287*, 1790-1800.
12. Dinter, J.; Mühlhaus, J.; Wienchol, C. L.; Yi, C.-X.; Nürnberg, D.; Morin, S.; Grütters, A.; Köhrle, J.; Schöneberg, T.; Tschöp, M., Inverse agonistic action of 3-

1
2
3
4
5
6
7
8
9
10
11
12
13
14
15
16
17
18
19
20
21
22
23
24
25
26
27
28
29
30
31
32
33
34
35
36
37
38
39
40
41
42
43
44
45
46
47
48
49
50
51
52
53
54
55
56
57
58
59
60

iodothyronamine at the human trace amine-associated receptor 5. *PLoS One* **2015**, *10*, e0117774-e0117774.

13. Chiellini, G.; Frascarelli, S.; Ghelardoni, S.; Carnicelli, V.; Tobias, S. C.; DeBarber, A.; Brogioni, S.; Ronca-Testoni, S.; Cerbai, E.; Grandy, D. K., Cardiac effects of 3-iodothyronamine: a new aminergic system modulating cardiac function. *FASEB J.* **2007**, *21*, 1597-1608.

14. Ghelardoni, S.; Suffredini, S.; Frascarelli, S.; Brogioni, S.; Chiellini, G.; Ronca-Testoni, S.; Grandy, D. K.; Scanlan, T. S.; Cerbai, E.; Zucchi, R., Modulation of cardiac ionic homeostasis by 3-iodothyronamine. *J. Cell. Mol. Med.* **2009**, *13*, 3082-3090.

15. Zucchi, R.; Accorroni, A.; Chiellini, G., Update on 3-iodothyronamine and its neurological and metabolic actions. *Front. Physiol.* **2014**, *5*, 402.

16. Braulke, L.; Klingenspor, M.; DeBarber, A.; Tobias, S.; Grandy, D.; Scanlan, T.; Heldmaier, G., 3-Iodothyronamine: a novel hormone controlling the balance between glucose and lipid utilisation. *J. Comp. Physiol. B* **2008**, *178*, 167-177.

17. Haviland, J.; Reiland, H.; Butz, D.; Tonelli, M.; Porter, W.; Zucchi, R.; Scanlan, T.; Chiellini, G.; Assadi-Porter, F., NMR-based metabolomics and breath studies show lipid and protein catabolism during low dose chronic T1AM treatment. *Obesity* **2013**, *21*, 2538-2544.

18. Manni, M. E.; De Siena, G.; Saba, A.; Marchini, M.; Landucci, E.; Gerace, E.; Zazzeri, M.; Musilli, C.; Pellegrini-Giampietro, D.; Matucci, R., Pharmacological effects of 3-iodothyronamine (T1AM) in mice include facilitation of memory acquisition and retention and reduction of pain threshold. *Br. J. Pharmacol.* **2013**, *168*, 354-362.

- 1
2
3
4
5
6
7
8
9
10
11
12
13
14
15
16
17
18
19
20
21
22
23
24
25
26
27
28
29
30
31
32
33
34
35
36
37
38
39
40
41
42
43
44
45
46
47
48
49
50
51
52
53
54
55
56
57
58
59
60
19. Klieverik, L. P.; Foppen, E.; Ackermans, M. T.; Serlie, M. J.; Sauerwein, H. P.; Scanlan, T. S.; Grandy, D. K.; Fliers, E.; Kalsbeek, A., Central effects of thyronamines on glucose metabolism in rats. *J. Endocrinol.* **2009**, *201*, 377-386.
20. Manni, M. E.; De Siena, G.; Saba, A.; Marchini, M.; Dicembrini, I.; Bigagli, E.; Cinci, L.; Lodovici, M.; Chiellini, G.; Zucchi, R., 3-Iodothyronamine: a modulator of the hypothalamus-pancreas-thyroid axes in mice. *Br. J. Pharmacol.* **2012**, *166*, 650-658.
21. Regard, J. B.; Kataoka, H.; Cano, D. A.; Camerer, E.; Yin, L.; Zheng, Y.-W.; Scanlan, T. S.; Hebrok, M.; Coughlin, S. R., Probing cell type-specific functions of Gi in vivo identifies GPCR regulators of insulin secretion. *J. Clin. Invest.* **2007**, *117*, 4034.
22. Dhillon, W.; Bewick, G.; White, N.; Gardiner, J.; Thompson, E.; Bataveljic, A.; Murphy, K.; Roy, D.; Patel, N.; Scutt, J., The thyroid hormone derivative 3-iodothyronamine increases food intake in rodents. *Diabetes Obes. Metab.* **2009**, *11*, 251-260.
23. Wood, W. J.; Geraci, T.; Nilsen, A.; DeBarber, A. E.; Scanlan, T. S., Iodothyronamines are oxidatively deaminated to iodothyroacetic acids in vivo. *ChemBioChem* **2009**, *10*, 361-365.
24. Hackenmueller, S. A.; Scanlan, T. S., Identification and quantification of 3-iodothyronamine metabolites in mouse serum using liquid chromatography-tandem mass spectrometry. *J. Chromatogr. A* **2012**, *1256*, 89-97.
25. Tan, E. S.; Groban, E. S.; Jacobson, M. P.; Scanlan, T. S., Toward deciphering the code to aminergic G protein-coupled receptor drug design. *Chem. Biol.* **2008**, *15*, 343-353.

- 1
2
3
4
5
6
7
8
9
10
11
12
13
14
15
16
17
18
19
20
21
22
23
24
25
26
27
28
29
30
31
32
33
34
35
36
37
38
39
40
41
42
43
44
45
46
47
48
49
50
51
52
53
54
55
56
57
58
59
60
26. Hart, M. E.; Suchland, K. L.; Miyakawa, M.; Bunzow, J. R.; Grandy, D. K.; Scanlan, T. S., Trace amine-associated receptor agonists: synthesis and evaluation of thyronamines and related analogues. *J. Med. Chem.* **2006**, *49*, 1101-1112.
27. Chiellini, G.; Apriletti, J. W.; Al Yoshihara, H.; Baxter, J. D.; Ribeiro, R. C.; Scanlan, T. S., A high-affinity subtype-selective agonist ligand for the thyroid hormone receptor. *Chem. Biol.* **1998**, *5*, 299-306.
28. Molander, G. A.; Elia, M. D., Suzuki-Miyaura cross-coupling reactions of benzyl halides with potassium aryltrifluoroborates. *J. Org. Chem.* **2006**, *71*, 9198-9202.
29. Barak, L. S.; Salahpour, A.; Zhang, X.; Masri, B.; Sotnikova, T. D.; Ramsey, A. J.; Violin, J. D.; Lefkowitz, R. J.; Caron, M. G.; Gainetdinov, R. R., Pharmacological characterization of membrane-expressed human trace amine-associated receptor 1 (TAAR1) by a bioluminescence resonance energy transfer cAMP biosensor. *Mol. Pharmacol.* **2008**, *74*, 585-594.
30. Espinoza, S.; Salahpour, A.; Masri, B.; Sotnikova, T. D.; Messa, M.; Barak, L. S.; Caron, M. G.; Gainetdinov, R. R., Functional interaction between trace amine-associated receptor 1 and dopamine D2 receptor. *Mol. Pharmacol.* **2011**, *80*, 416-25.
31. Ghelardoni, S.; Chiellini, G.; Frascarelli, S.; Saba, A.; Zucchi, R., Uptake and metabolic effects of 3-iodothyronamine in hepatocytes. *J. Endocrinol.* **2014**, *221*, 101-110.
32. Moro, S.; Deflorian, F.; Bacilieri, M.; Spalluto, G., Ligand-based homology modeling as attractive tool to inspect GPCR structural plasticity. *Curr. Pharm Des.* **2006**, *12*, 2175-2185.

- 1
2
3
4
5
6
7
8
9
10
11
12
13
14
15
16
17
18
19
20
21
22
23
24
25
26
27
28
29
30
31
32
33
34
35
36
37
38
39
40
41
42
43
44
45
46
47
48
49
50
51
52
53
54
55
56
57
58
59
60
33. Cichero, E.; Espinoza, S.; Gainetdinov, R. R.; Brasili, L.; Fossa, P., Insights into the structure and pharmacology of the human trace amine-associated receptor 1 (hTAAR1): homology modelling and docking studies. *Chem. Biol. Drug Des.* **2013**, *81*, 509-516.
34. Cichero, E.; D'Ursi, P.; Moscatelli, M.; Bruno, O.; Orro, A.; Rotolo, C.; Milanesi, L.; Fossa, P., Homology modeling, docking studies and molecular dynamic simulations using graphical processing unit architecture to probe the type-11 phosphodiesterase catalytic site: a computational approach for the rational design of selective inhibitors. *Chem. Biol. Drug Des.* **2013**, *82*, 718-731.
35. Rosenbaum, D. M.; Zhang, C.; Lyons, J. A.; Holl, R.; Aragao, D.; Arlow, D. H.; Rasmussen, S. G.; Choi, H.-J.; DeVree, B. T.; Sunahara, R. K., Structure and function of an irreversible agonist- β 2 adrenoceptor complex. *Nature* **2011**, *469*, 236-240.
36. Bairoch, A.; Apweiler, R., The SWISS-PROT protein sequence database and its supplement TrEMBL in 2000. *Nucleic Acids Res.* **2000**, *28*, 45-48.
37. Berman, H. M.; Westbrook, J.; Feng, Z.; Gilliland, G.; Bhat, T.; Weissig, H.; Shindyalov, I. N.; Bourne, P. E., The protein data bank. *Nucleic Acids Res.* **2000**, *28*, 235-242.
38. Levitt, M., Accurate modeling of protein conformation by automatic segment matching. *J.Mol. Biol.* **1992**, *226*, 507-533.
39. Fechteler, T.; Dengler, U.; Schomburg, D., Prediction of protein three-dimensional structures in insertion and deletion regions: a procedure for searching data bases of representative protein fragments using geometric scoring criteria *J.Mol. Biol.* **1995**, *253*, 114-131.

- 1
2
3
4
5
6
7
8
9
10
11
12
13
14
15
16
17
18
19
20
21
22
23
24
25
26
27
28
29
30
31
32
33
34
35
36
37
38
39
40
41
42
43
44
45
46
47
48
49
50
51
52
53
54
55
56
57
58
59
60
40. Cornell, W. D.; Cieplak, P.; Bayly, C. I.; Gould, I. R.; Merz, K. M.; Ferguson, D. M.; Spellmeyer, D. C.; Fox, T.; Caldwell, J. W.; Kollman, P. A., A second generation force field for the simulation of proteins, nucleic acids, and organic molecules *J. Am. Chem. Soc.* **1996**, *118*, 2309-2309.
41. Reese, E. A.; Norimatsu, Y.; Grandy, M. S.; Suchland, K. L.; Bunzow, J. R.; Grandy, D. K., Exploring the determinants of trace amine-associated receptor 1's functional selectivity for the stereoisomers of amphetamine and methamphetamine. *J. Med. Chem.* **2014**, *5*, 378-390.
42. Salahpour, A.; Espinoza, S.; Masri, B.; Lam, V.; Barak, L. S.; Gainetdinov, R. R., BRET biosensors to study GPCR biology, pharmacology, and signal transduction. *Front. Endocrinol.* **2012**, *3*, 105
43. Zucchi, R.; Ronca-Testoni, S.; Yu, G.; Galbani, P.; Ronca, G.; Mariani, M., Effect of ischemia and reperfusion on cardiac ryanodine receptors-sarcoplasmic reticulum Ca²⁺ channels. *Circ. Res.* **1994**, *74*, 271-280.

Table of content graphic

